




Research Article

Integration of Wind Systems with SVC and STATCOM during Various Events to Achieve FRT Capability and Voltage Stability: Towards the Reliability of Modern Power Systems

Mohamed Metwally Mahmoud ¹, Hossam S. Salama,^{1,2} Mohit Bajaj ^{3,4,5},
Mohamed M. Aly,¹ Istvan Vokony,² Syed Sabir Hussain Bukhari,⁶
Daniel Eutyche Mbadjoun Wapet ⁷ and Abdel-Moamen M. Abdel-Rahim⁸

¹Electrical Engineering Department, Faculty of Energy Engineering, Aswan University, Aswan 81528, Egypt

²Department of Electric Power Engineering, Budapest University of Technology and Economics, Budapest 1111, Hungary

³Department of Electrical Engineering, Graphic Era (Deemed to be University), Dehradun 248002, India

⁴Graphic Era Hill University, Dehradun 248002, India

⁵Applied Science Research Center, Applied Science Private University, Amman 11931, Jordan

⁶School of Electrical and Electronics Engineering, Chung-Ang University, Dongjak-gu, Seoul 06974, Republic of Korea

⁷National Advanced School of Engineering, Université de Yaoundé I, Yaoundé, Cameroon

⁸Department of Electrical Engineering, Faculty of Energy Engineering, Aswan University, Aswan, Egypt

Correspondence should be addressed to Mohamed Metwally Mahmoud; metwally_m@aswu.edu.eg
and Daniel Eutyche Mbadjoun Wapet; eutychedan@gmail.com

Received 31 August 2022; Revised 3 November 2022; Accepted 30 November 2022; Published 15 February 2023

Academic Editor: Akshay Kumar Saha

Copyright © 2023 Mohamed Metwally Mahmoud et al. This is an open access article distributed under the Creative Commons Attribution License, which permits unrestricted use, distribution, and reproduction in any medium, provided the original work is properly cited.

FACTS tools in modern power systems provide a vital solution to the problems of voltage deviation and fault ride-through (FRT) capability in electrical power systems especially during the integration of wind power. Many distinct journals highlight that the wind-driven squirrel cage generator (SCIG) still accounts for around 15% of operating wind generators so far. To enhance voltage stability and FRT capacity, this paper recommends a cost-effective static VAR compensator (SVC) which has a size rating of six MVAR, and this improves the efficiency of the electrical power system. Different events are considered in this study such as high turbulent wind speed, low turbulent wind speed, unsymmetrical faults, and symmetrical faults to validate the suggested option. Moreover, the suggested solution is compared with the static synchronous compensator (STATCOM) and a fixed capacitor to ensure that during the studied wind speed profiles and faults, voltage stability, reactive power consumption, and FRT capability are realized. An overall comparison among them is performed under all studied scenarios to summarize their benefits and impacts. The simulated results show the effectiveness and superiority of SVC in improving the operation of an integrated wind system based on a grid-linked SCIG and the performance of the power system. The modeling of SCIG, SVC, and STATCOM is designed by MATLAB/Simulink toolbox.

1. Introduction

The high penetration ratio of sustainable energy production systems into the electrical grids in the world has been conspicuous these days. Many countries aim to use natural resources to gradually replace conventional power plants, which rely mainly on fossil fuel consumption, with cleaner sources a chal-

lenge. World renewable production capacity was 3064 GW at the end of 2021. With a capacity of 1,230 GW, hydropower is reported for the biggest portion of the worldwide total. The remaining energy was split equally between solar and wind power, with capabilities of 849 and 825 GW, respectively. Other renewable sources counted in 524 MW of marine energy, 143 GW of biofuel, and 16 GW of geothermal [1–3].

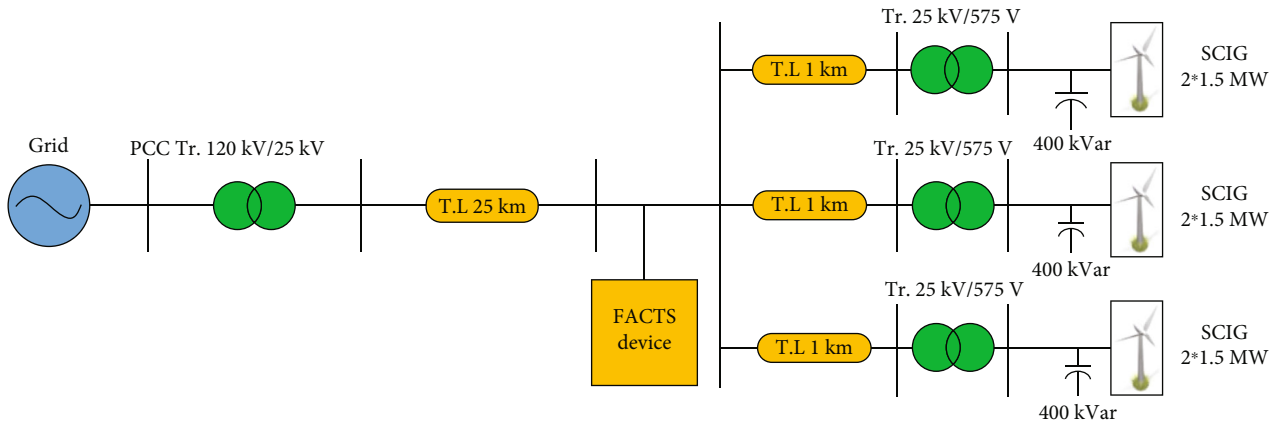


FIGURE 1: Scheme of the system model.

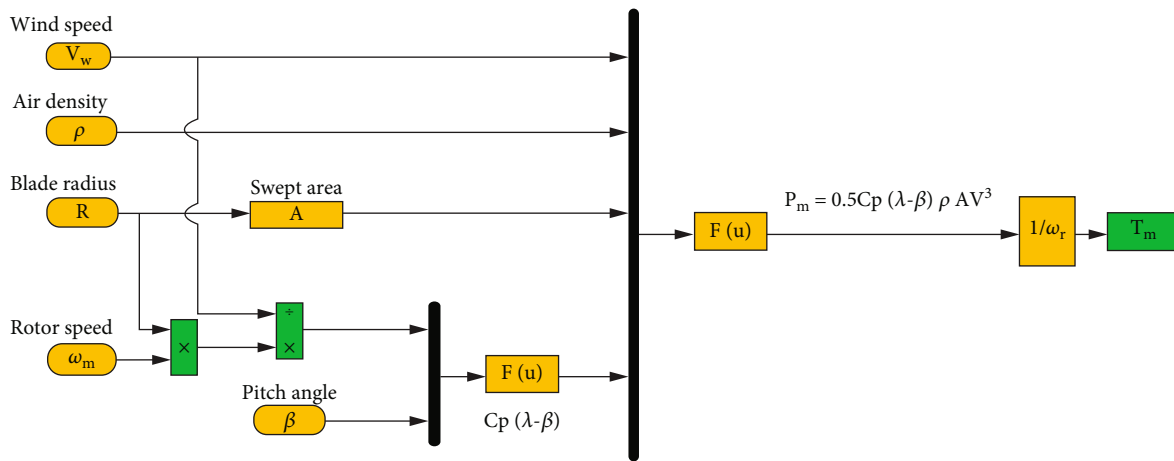


FIGURE 2: Modeling of the wind turbine.

Nevertheless, the high usage of an unpredictable and intermittent source like wind presents challenges of reliability and stability within the grid that need to be appropriately studied [4–6].

Many types of research have already been done to assess the effect of an immense amount of wind power incorporation into the grid [7–10]. To keep the quality of the power supply, frequency and voltage regulation as key factors must be taken into consideration, whereas a balance between the generation of real and reactive power (Q) flow and the demand for load must be maintained so that the reliability of the power grid is not threatened. In the earliest periods of wind energy generation development, the industry was dominated by fixed-speed wind generators (FSWGs) fitted with a squirrel cage induction generator (SCIG) [11–14]. By now, new and improved wind turbine (WT) technologies have appeared, like the doubly fed induction generator (DFIG) [15–17] and the permanent magnet synchronous generator (PMSG) [18–20]. In spite of this, the SCIG remains a determining factor in the global wind farm (WF) [21].

Nevertheless, the use of this technology has faced many problems. The SCIG provides a simple system with a direct connection of the stator windings to the power grid. Short circuit was done on SCIG rotor windings and is not electrically accessible. Such a system does not contain any power

converter or specialized apparatus in the generator itself to enable the control of real and Q . Therefore, the stator currents have to confirm that the grid-imposed frequency can only be accomplished with a very small variability margin in the WT's rotational speed [22, 23]. Owing to its configuration, the SCIG needs some Q in the windings of the stators to establish the magnetic field. This consumption of SCIG is normally minimized when it works in steady-state cases using compensating capacitors. Such capacitors are probably linked to modules or detached to suit changed power levels [24].

This behavior develops smoothly less acceptable when there is a grid disturbance. During voltage dips, the WT's active power output drops rapidly, while it still needs grid-to-generator Q support. It aggravates the impact of the fault on the voltage, normally causing either overspeed or undervoltage to cause the FSWGs to trip [5, 24, 25]. This helps restore voltage stability; however, this reduces the charging of the active power supply, which impedes the power balance of the grid.

Thereafter, newly developed grid codes should be achieved in case of high-income countries' wind energy penetration [26–28] set low voltage ride-through (LVRT) capabilities forcing FSWG to stay in service during voltage decreases with identified

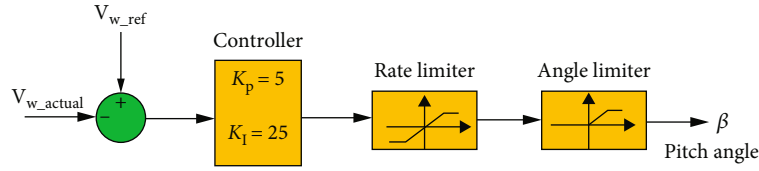


FIGURE 3: Pitch angle control.

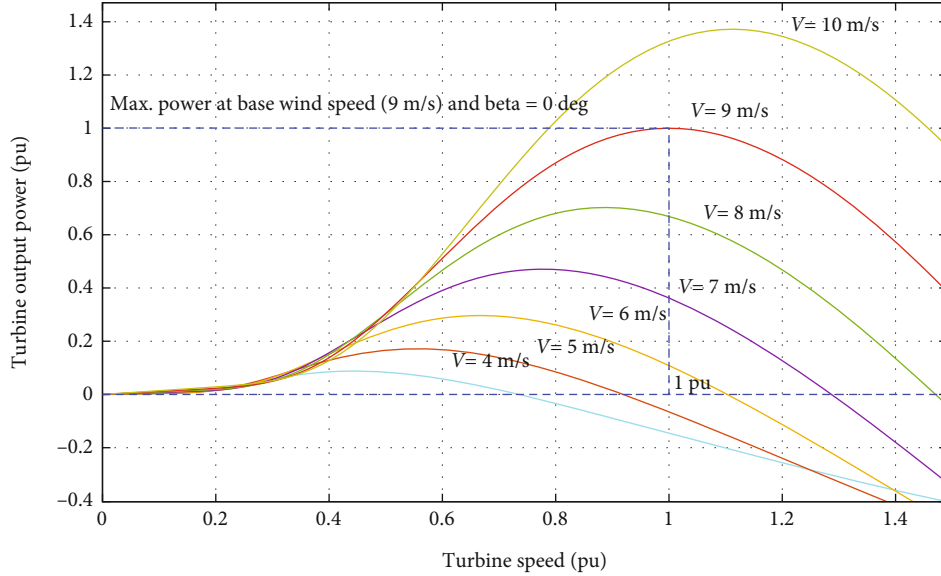


FIGURE 4: WT characteristics under varying different wind speeds.

TABLE 1: Rated parameters for 1.5 MW wind-driven SCIG.

Parameter	Value
Rated power	1.5 (MW)
Stator resistance	0.00483 (pu)
Stator inductance	0.1248 (pu)
Rotor resistance	0.004377 (pu)
Rotor inductance	0.1791 (pu)
Mutual inductance	6.77 (pu)
Pole pairs	3
Frequency	60 (Hz)
Stator voltage	575 (V)
Friction factor	0.01 (pu)
Inertia	5.04 (s)

TABLE 2: Wind turbine parameters.

Parameter	Value
Number of blades	3
Density of air	1.22 (kg.m ⁻³)
Nominal wind speed	9 (m.s ⁻¹)

characteristics and deliver a certain quantity of Q to support the recovery of voltage. Still, the SCIG cannot accomplish this function on its own. Additional types of equipment are required; therefore, it is necessary to enable this knowledge to fulfill the requirements of execution. A significant role has been played here by flexible AC transmission system (FACTS) tools. Many distinguishing tools can be categorized under FACTS like static synchronous compensator (STATCOM) and static VAR compensator (SVC), which serve as an appropriate key to the problems of Q and voltage regulation of FSWG [29–32]. Such tools

will connect the FSWG to achieve the superiority of the energy supplied to the grid and to realize the LVRT capabilities provided by new network codes [33–35]. STATCOM and SVC may be specified as parallel-linked tools with the SCIG exit terminals according to their installation.

The literature has dealt with the integration of STATCOM and SVC into WF. The LVRT improvement of FSWG using STATCOM [36–38] and their ability to fulfill grid code necessities have been given particular attention. In addition, an improved design was provided in [39–41], wherever energy storage units were added to the STATCOM scheme to permit real power flow management and enhance power system frequency control [42]. SVC and STATCOM have different characteristics with regard to their configuration and controllability. Thus, the different actions of these tools are predictable under the same working conditions. Nevertheless, there are no appropriate sources in which comparisons are made between these two technologies. Henceforth, this aspect is well-thought-out here, mainly concentrated on their behavior along with the grid-connected FSWG.

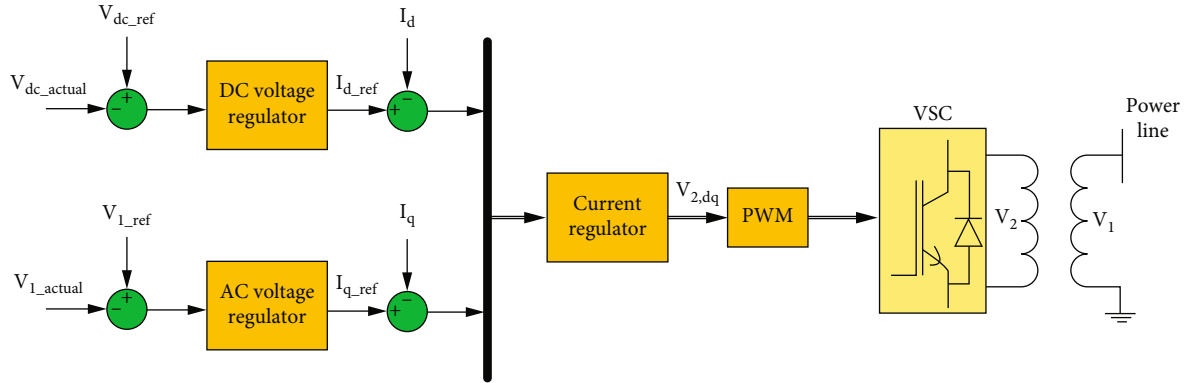


FIGURE 5: The schematic figure of STATCOM and its control.

TABLE 3: The parameter of the PID controller for STATCOM.

Controllers	K_p	K_I	K_D
DC voltage regulator	5	1000	0
AC voltage regulator	0.0001	0.02	0
Current regulator	0.3	10	0.22

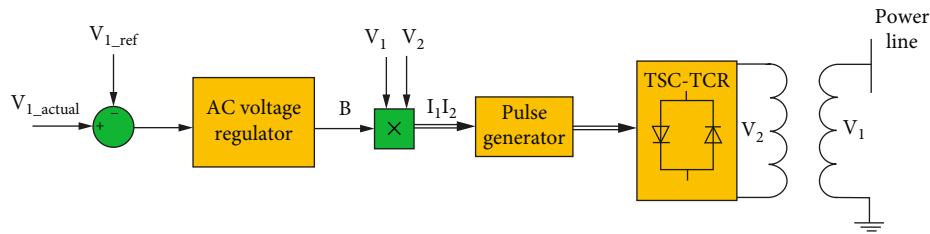


FIGURE 6: Schematic diagram of SVC and its control.

TABLE 4: Parameters of the PID controller for SVC.

AC voltage regulator gains	K_p	K_I	K_D
Values	0	300	0

The literature has suggested a number of configurations and control schemes for WF systems outfitted with FACTS tools. The FSWGs did not test in the literature with high, fluctuating, and gusty wind speeds and severe faults. Additionally, the WG's dynamic performance was unaddressed in terms of pitch control and rotation speed. The FACTS paradigm, in which SVC or STATCOM can service WGs, is one of the acceptable choices. However, this paper's goal is to examine the dynamic performance of a suggested design and determine the appropriate size of FACTS that can be connected and used independently in any location on the electric grid, rather than just as a component of a WF. Such dispersed configurations can be installed at the grid's weaker nodes to increase the system's dependability and stability.

This paper examines the dynamic behavior of SCIG-based WF connected with STATCOM and SVC under regular and irregular grid conditions. The integration of FACTS tools with grid-connected FSWG has been done which leads to compensation of the SCIG and enhances grid stability during instability events. Thus, two separate configurations

were provided conferring to the incorporated FACTS, i.e., SVC and STATCOM. Transient stability scenarios are performed in MATLAB/Simulink under different operating conditions to test the models' dynamic response to grid faults. The following are the key contributions of this article:

- (i) A grid-tied wind system combined of six FSWGs is assessed and tested under different harsh operating events (high turbulent wind speed, low turbulent wind speed, single phase fault, double line fault, and three phase fault)
- (ii) Application of FACTS tools (SVC and STATCOM) in grid-connected wind systems for enhancing the reliability of recent power systems via achieving FRT capability and voltage stability
- (iii) The maximal produced power during changes in wind speed may be obtained with the suggested SVC, the injected Q into the grid is readily managed, and FRT conditions can be successfully met
- (iv) The applied control for the FACTS' appropriate operation is provided and discussed
- (v) The different behaviors of the proposed and efficient tools (SVC and STATCOM) that eradicate

TABLE 5: Prices of FACTS devices.

FACTS tools	Installation cost included	Cost (\$/kVAR)			
		100 MVAR	200 MVAR	300 MVAR	400 MVAR
SVC	Yes	100	80	70	60
	No	60	50	45	40
STATCOM	Yes	130	115	110	100
	No	90	75	68	60

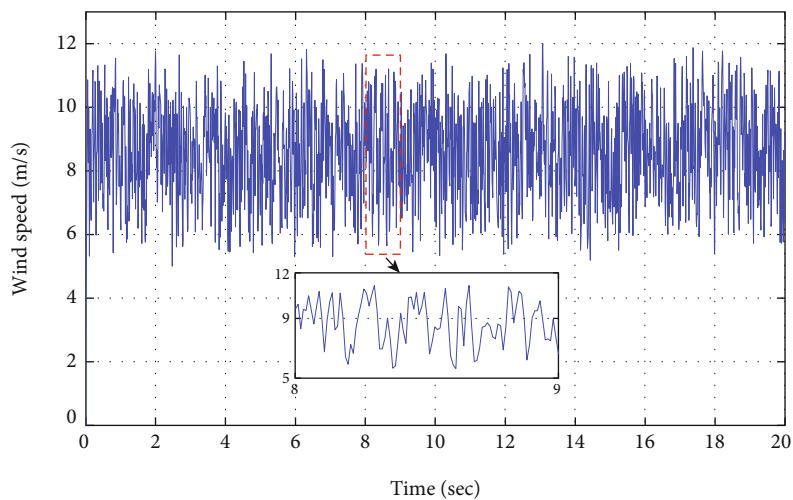


FIGURE 7: The high turbulent wind speed.

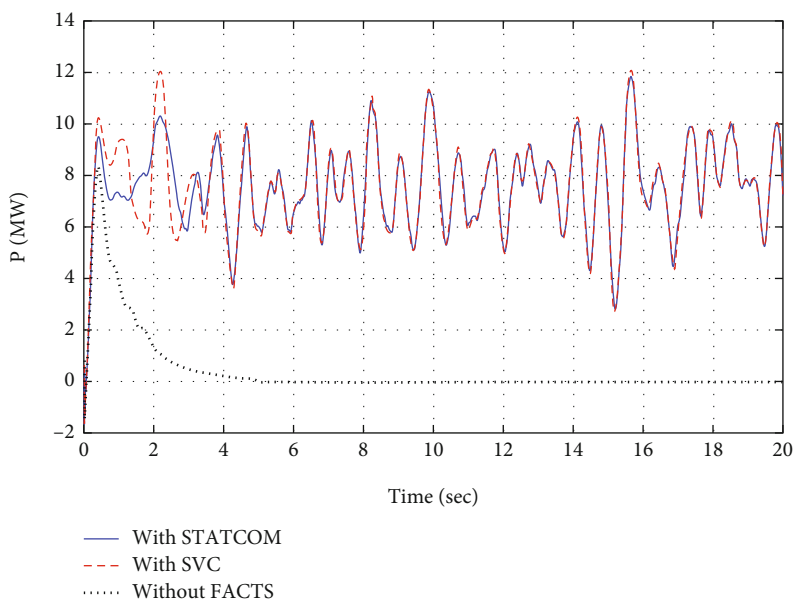


FIGURE 8: The real power at PCC.

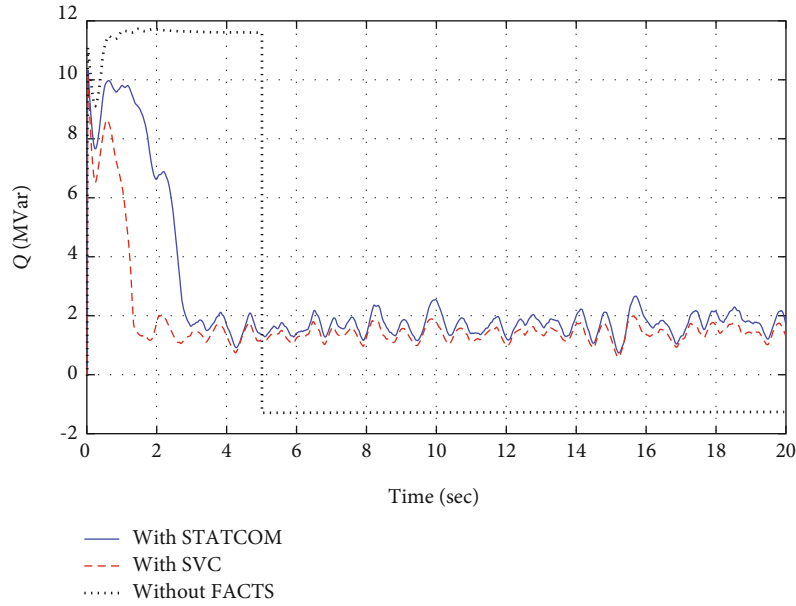


FIGURE 9: The Q at PCC.

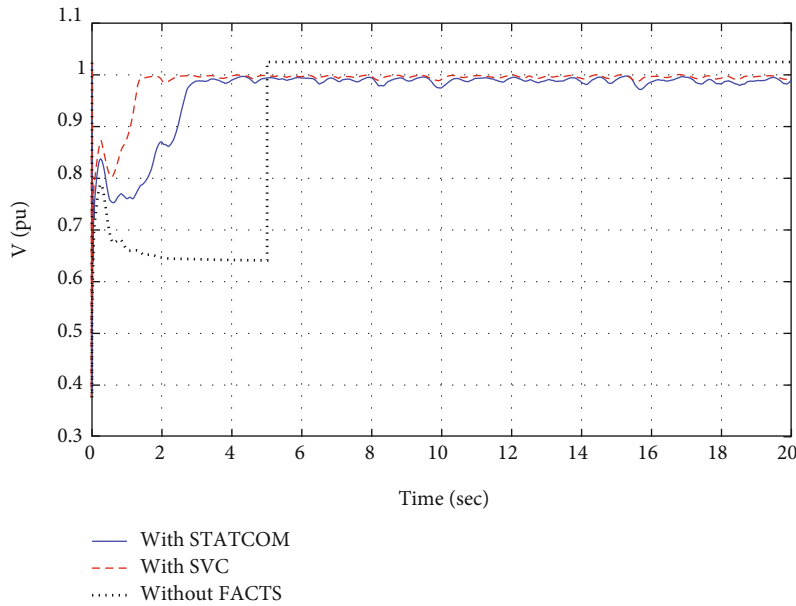


FIGURE 10: Voltage response at the PCC.

the limitations and drawbacks of fixed capacitors and improve the operation of the WF system are analyzed under five operating conditions

- (vi) The studied wind speed profiles aim to assess the role of SVC and STATCOM in mitigating the high variability in wind speed through injecting the needed Q. In addition, the presence of proposed FACTS enables the pitch control system to do its function smoothly
- (vii) The outcomes are reported and a comparative analysis is conducted among all the suggested configurations

This paper is structured as follows. Section 2 offers a brief depiction of the WF. Models of the FACTS are described in Section 3. Section 4 describes and addresses simulations. Lastly, the conclusions drawn from the study are described in Section 5.

2. Wind Farm Description

The WF is simulated in MATLAB/Simulink and tested with various FACTS tools to test its behavior. It contains three similar branches linked to a common node, which is considered to

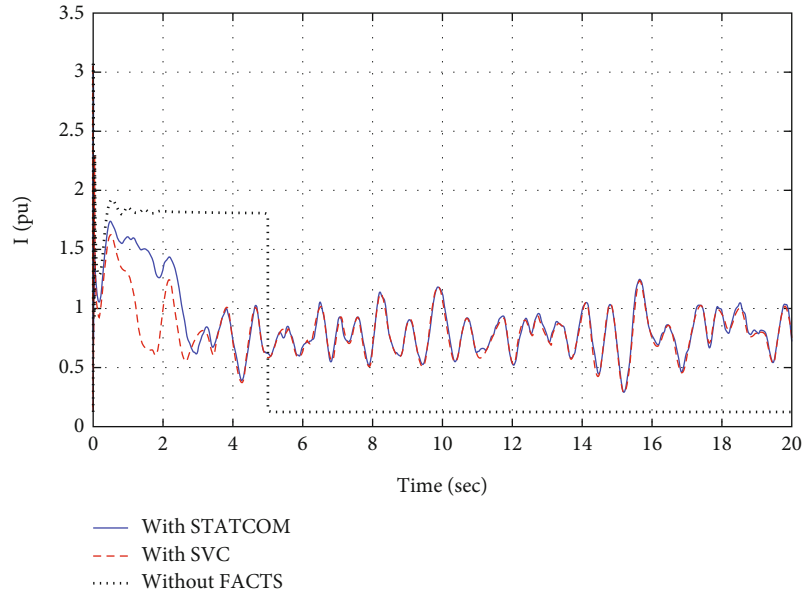


FIGURE 11: The system’s current response.

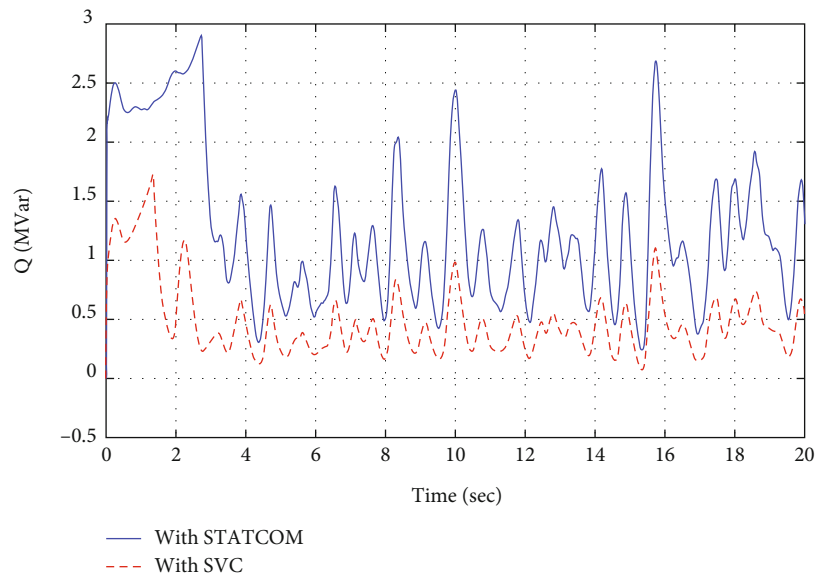


FIGURE 12: The Q of STATCOM and SVC.

be the wind farm’s production terminal. In addition, each branch contains two SCIG-equipped fixed-speed wind turbines. The SCIG output capacity is 1.5 MW. Therefore, a full average WF capacity of 9 MW is generated from three divisions of 3 MW each. In addition, each pair of wind generators (WG) linked to the same outlet has a 400 kVAR reactive capacitor at their output. The WF scheme is depicted in Figure 1. A voltage transformer (VT) is also needed to increase the output of the 575 V SCIG to 25 kV, which is the voltage used throughout the WF system. Furthermore, among the three divisions of the WF, three of VTs 575 V/25 kV of 4 MVA rated power are installed. In addition, the pi-model

has been used to implement a 1 km long transmission line to account for power loss from the output of the transformer to the specific point.

In each of the three divisions, the structure is replicated. The same node also serves as the linking port for those tools in cases where FACTS is applied. An additional branch is attached to the WF’s common node in parallel with one of the FACTS tools and the rest of the power line to the common coupling point (PCC). Therefore, if no FACTS are well-thought-out, this dimension necessity is omitted and together nodes must be associated with the scheme shown in Figure 1. Using the FACTS tools, the pi-model of a

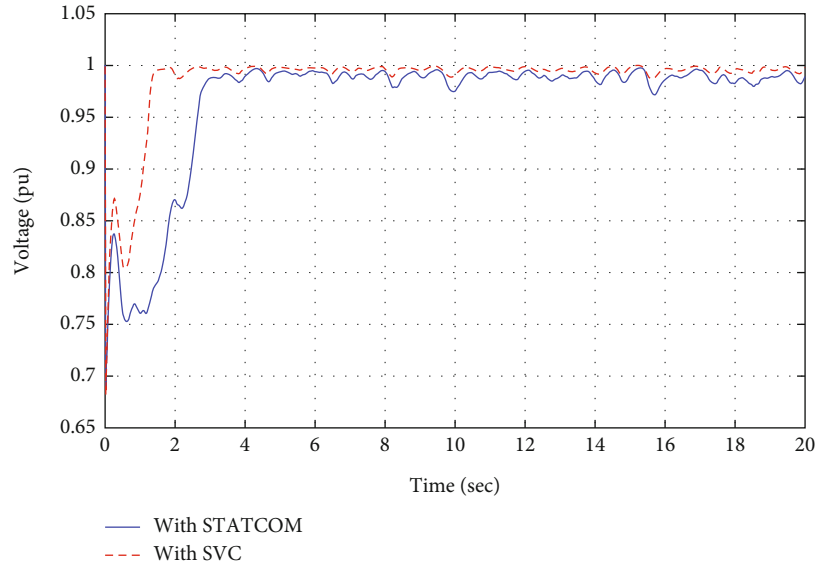


FIGURE 13: A voltage of the SVC and STATCOM.

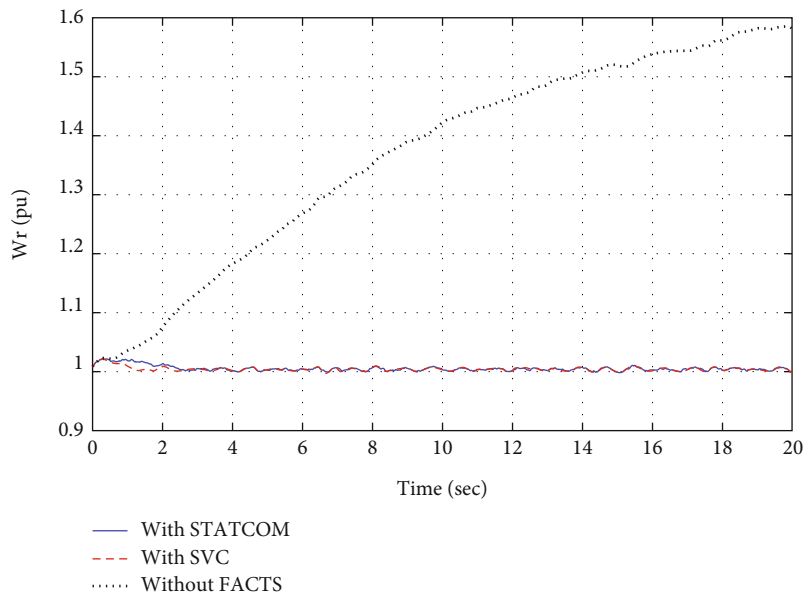


FIGURE 14: The SCIG speed variation.

25 km long transmission line (TL) connects the WF to a VT that increases the voltage from 25 kV to 120 kV that the PCC requires to a 47 MVA grid. Lastly, the grid is typically designed to use a three-phase AC supply which generates a steady AC signal on the PCC for both amplitude and frequency.

2.1. *Modeling of WEGs.* The responsibility of the wind turbine is to change the kinetic energy to mechanical energy. The modeling of wind turbines has been discussed in detail in [43–45]. In the equation below, C_p is the coefficient of performance which is related to β (blade pitch angle) and

λ (tip speed ratio). For SCIG, C_p is specified by

$$C_p(\lambda, \beta) = 0.5176 \left(\frac{116}{\lambda i} - 0.4\beta - 5 \right) \exp^{-21/\lambda i} + 0.0068\lambda, \tag{1}$$

$$\frac{1}{\lambda i} = \frac{1}{\lambda + .08\beta} - \frac{.035}{\beta^3 + 1}, \tag{2}$$

$$\lambda = \frac{\omega_m * R}{V_{wind}}. \tag{3}$$

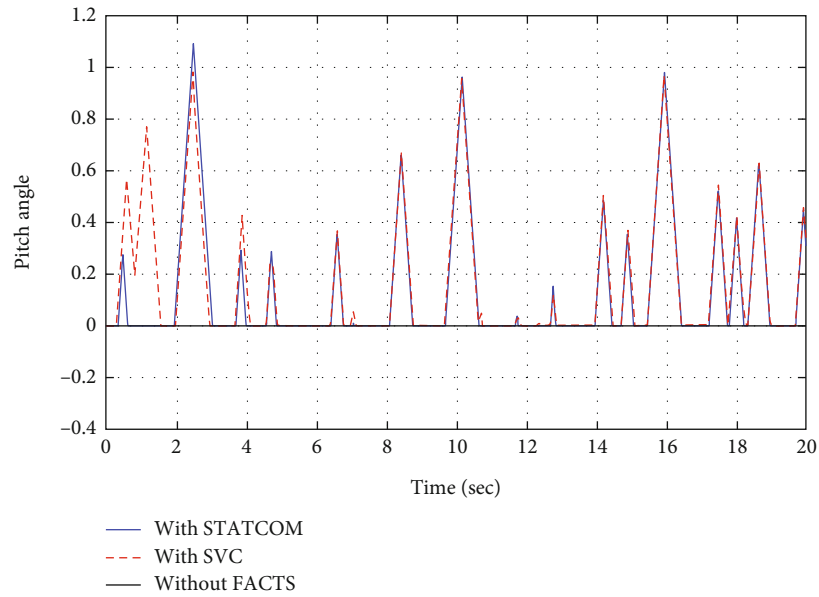


FIGURE 15: Pitch angle control response.

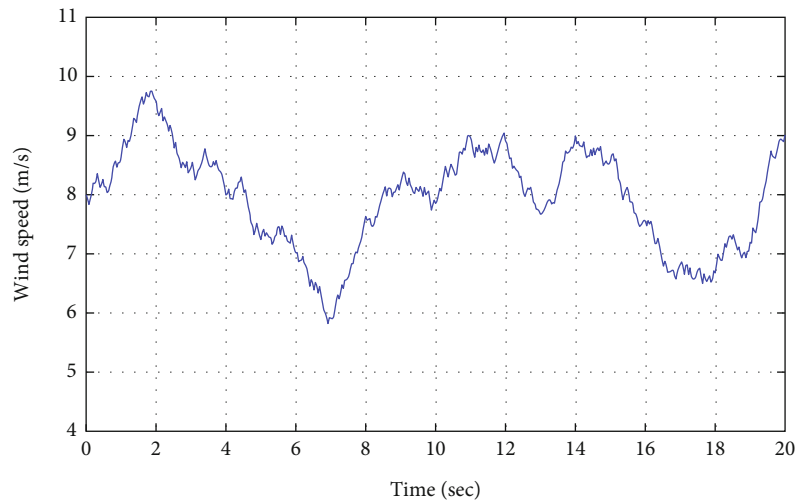


FIGURE 16: Realistic wind speed.

Equation (4) shows the turbine's mechanical output power.

$$P_m = 0.5c_p \rho A (V_{\text{wind}})^3, \quad (4)$$

where ρ is the air density, A is the turbine swept area, and V_{wind} is the wind speed.

The value of ω_m can be obtained from equation (3).

$$T_{\text{tur}} = \frac{P_m}{\omega_m}, \quad (5)$$

$$T_{\text{tur}} = J_{\text{eq}} \frac{d\omega_m}{dt} + B_{\text{eq}} \omega_m + T_e.$$

The variables T_{tur} , J_{eq} , B_{eq} , and T_e are turbine torque,

total equivalent inertia of the turbine, damping coefficient, and the electromagnetic torque of the generator, respectively. The modeling of wind turbines is shown in Figure 2. Pitch angle controller (PAC) is one of the software solutions that assist in LVRT by keeping the generator operated at rated wind speeds. When the wind turbine is exposed to wind gusts, the pitch angle increases to reduce C_p , and therefore, the output power decreases where the pitch angle equals zero at normal wind speeds. This is illustrated in Figure 3. The characteristics of the wind turbine under different wind velocities are depicted in Figure 4.

2.2. Modeling of SCIG. A fourth-order model describes the dynamic model of the SCIG according to the equations below. The rotor and stator voltages in a reference frame

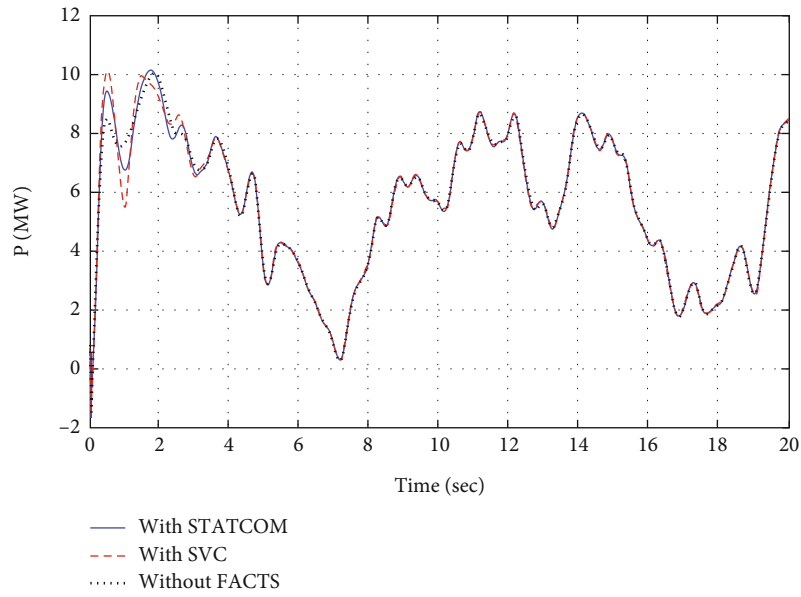


FIGURE 17: Active power at the PCC.

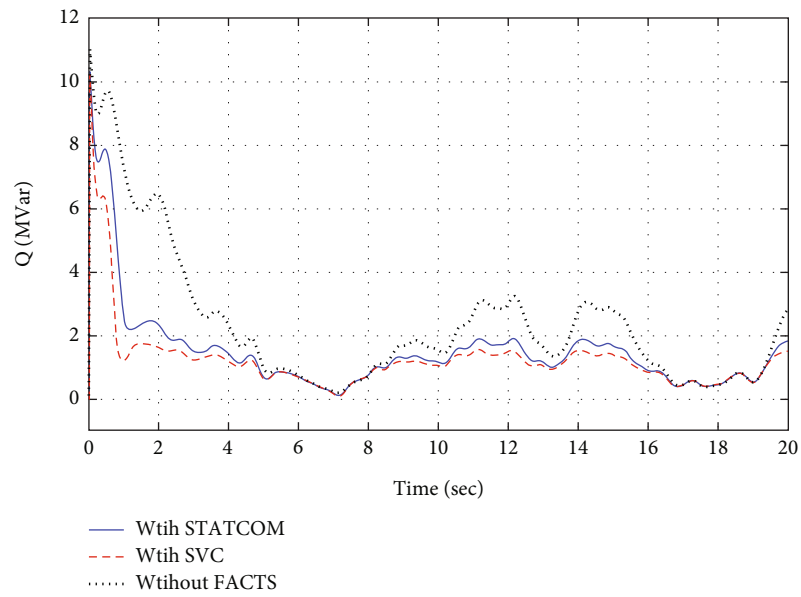


FIGURE 18: The Q at the PCC.

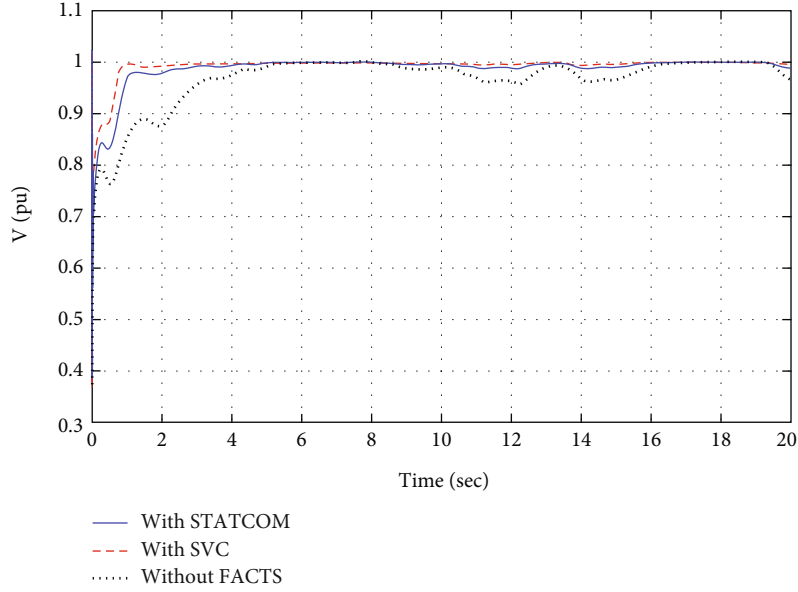


FIGURE 19: Voltage response at the PCC.

of direct (d) and quadrature (q) through the park transformation are indicated by the SCIG [43].

$$V_{qs} = R_s I_{qs} + P \lambda_{qs} + \omega \lambda_{ds},$$

$$V_{ds} = R_s I_{ds} + P \lambda_{ds} - \omega \lambda_{qs},$$

$$V_{qr} = R_r I_{qr} + P \lambda_{qr} + (\omega - \omega_r) \lambda_{dr} = 0,$$

$$V_{dr} = R_r I_{dr} + P \lambda_{dr} - (\omega - \omega_r) \lambda_{qr} = 0,$$

$$\begin{bmatrix} ids \\ iqs \\ idr \\ iqr \end{bmatrix} = \frac{1}{D1} \begin{bmatrix} Lr & 0 & -Lm & 0 \\ 0 & Lr & 0 & -Lm \\ -Lm & 0 & Ls & 0 \\ 0 & -Lm & 0 & Ls \end{bmatrix} \begin{bmatrix} \lambda ds \\ \lambda qs \\ \lambda dr \\ \lambda qr \end{bmatrix},$$

$$\lambda_{ds} = \frac{(V_{ds} - R_s I_{ds} + \omega \lambda_{ds})}{S},$$

$$\lambda_{qs} = \frac{(V_{qs} - R_s I_{qs} - \omega \lambda_{ds})}{S},$$

$$\lambda_{dr} = \frac{(V_{dr} - R_r I_{dr} + (\omega - \omega_r) \lambda_{qr})}{S},$$

$$\lambda_{qr} = \frac{(V_{dr} - R_r I_{qr} - (\omega - \omega_r) \lambda_{dr})}{S},$$

$$D1 = L_s L_r - (L_m)^2,$$

$$T_e = 1.5P(I_{qs} \lambda_{ds} - I_{ds} \lambda_{qs}).$$

(6)

The wind-driven SCIG is equipped with a pitch angle controller which restricts the capture of mechanical energy to prevent hazardous processes at strong wind speeds. The parameters used in modeling are voltage (V), current (I), resistance (R), number of poles (P), rotor angular speed (ω_r), flux linkage (λ), electromagnetic torque (T_e), and

inductance (L), where subindexes r and s stand for rotor and stator, respectively. The SCIG and wind turbine parameters are listed in Tables 1 and 2, respectively.

3. Modeling of FACTS

The FACTS is defined as a system consisting of a static device based on power electronic theory and utilized in the AC transmission power network to improve reliability, controllability, and power transfer capability. The FACTS family contains many devices with different operating principles and configurations. STATCOM and SVC are used in this work to improve a wind farm's grid-connecting capabilities and power system stability.

3.1. STATCOM Modeling. The STATCOM is a converter-based, parallel-connected switching tool used by reactive power injection or absorption to regulate voltage and electrical power flows [46–49]. The STATCOM is a parallel static synchronous generator that can change the amount of reactive power as capacitive or inductive, according to the IEEE definition for FACTS devices. STATCOM has a lot of merits like a fast response, high accuracy, small size, and perfect dynamic characteristics during variable operating conditions. This component contains a voltage-sourced converter, which produces at its output a regulated AC voltage using a coupling transformer, a DC capacitor, and semiconductor switches mainly insulated gate bipolar transistors (IGBT). It will be modeled as a voltage-controlled source of current, the value of which is defined according to the primary and secondary voltages of the coupling transformer. A primary voltage is measured directly at the contact port in STATCOM, while the secondary voltage is calculated indirectly. STATCOM's primary role is to produce a sinusoidal waveform at the PCC and control reactive current flow.

Throughout the control system introduced (Figure 5), the converter current quadrature portion (in a $d-q$ reference frame) regulates the transformer's primary voltage to

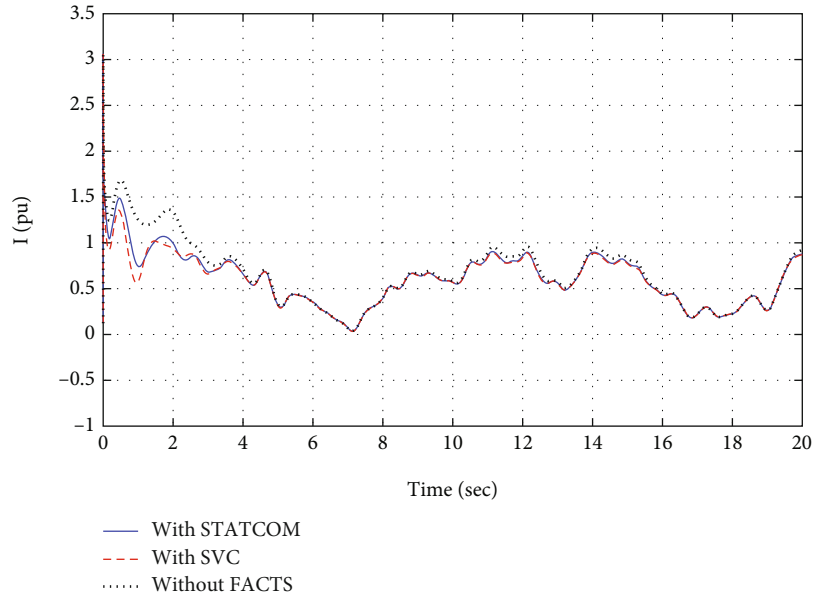


FIGURE 20: System current response.

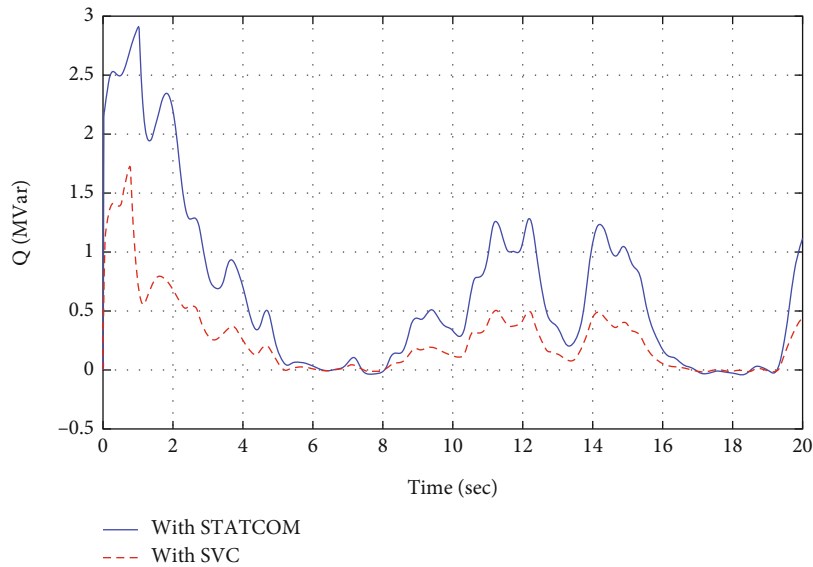


FIGURE 21: The Q of SVC and STATCOM.

its reference, and hence, the Q exchange with the network, using a PI controller and taking into account the device's droop characteristic. On the other hand, using a PI controller, the direct portion of the converter current is applied to adjust the DC voltage on the capacitor lateral of the converter and then the real power flow in the converter. Instead, with together current references, the secondary voltage $d-q$ components are applied by a current regulator, which is sent to a pulse width modulation (PWM) generating the switching signals for the electronic devices that convert electricity. The Q is controlled by the voltage magnitude of the converter output voltage and the AC main voltage. Its amount is given by equation (7). If V_2 is lower than V_1 , Q is flowing

from V_1 to V_2 (STATCOM is consuming reactive power). If V_2 is higher than V_1 , Q is flowing from V_2 to V_1 (STATCOM is injecting Q). Table 3 lists the value of proportional integral derivative (PID) controllers for the STATCOM.

$$Q = \frac{V_1(V_1 - V_2)}{X}. \quad (7)$$

3.2. SVC Modeling. Recently a shunt-connected SVC is equipped with a grid to enhance voltage stability and control the power flow in power systems. Compared to STATCOM, this device allows the electrical system which is attached to the Q exchange. Furthermore, it operates in a different

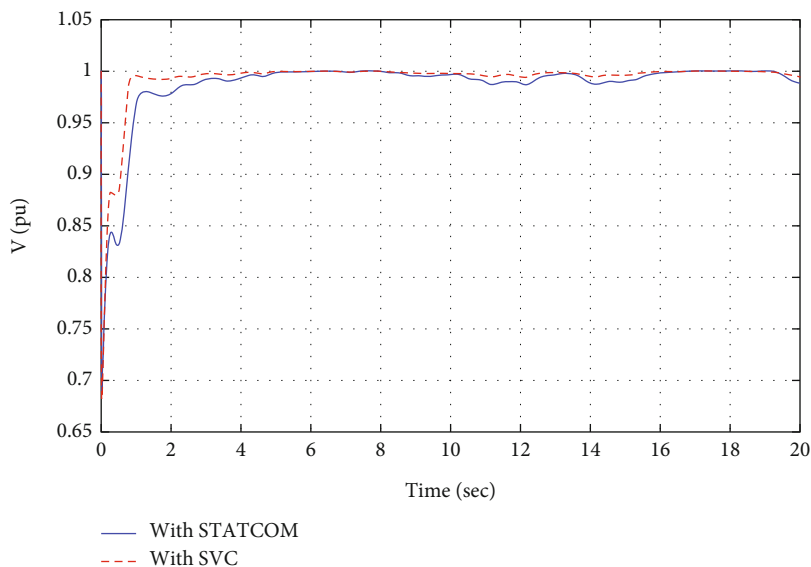


FIGURE 22: A voltage of SVC and STATCOM.

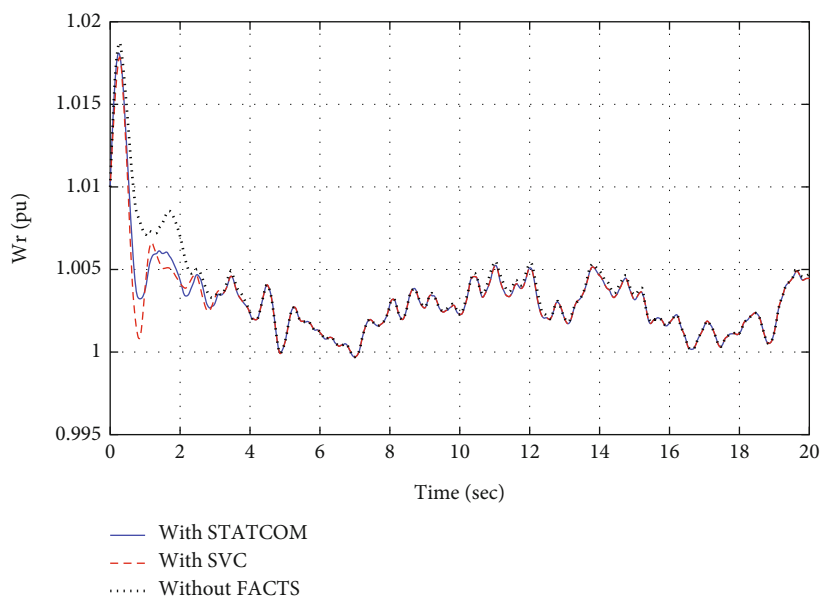


FIGURE 23: SCIG speed variation.

manner from the STATCOM system. In SVC, Q injection or absorption is achieved by means of a varying admittance that can change from inductive to capacitive depending on the controller's needs [46–48]. Thyristor-switched/operated capacitors and reactors can achieve this performance.

Figure 6 depicts a control system using a single loop PI-based controller, where the input is the error allusion between the calculated voltage at the SVC terminals and their references, and the variable susceptance is dynamically measured at the output. The susceptance is compounded by the voltage measured and changed into currents. Such currents are therefore measured to account for the voltage variability by variable susceptance and are pumped into the SVC-controlled power system. Here, the overall inductive

and capacitive limits of the susceptance are based on the Q compensation limits of this unit. Table 4 lists the value of PID controllers for the SVC.

3.3. Price-Effective FACTS Research. The basic rule is that business and financial interests come from utility management, and therefore, it is appropriate to carefully examine the cost-benefit analysis of various system changes. FACTS system costs consist of two basic components: the initial cost of installation and the cost of operation and maintenance. Due to the various factors that must be considered when choosing FACTS equipment such as power rating, device type, system voltage, system requirement, ecological conditions, and administrative prerequisites, it is difficult to

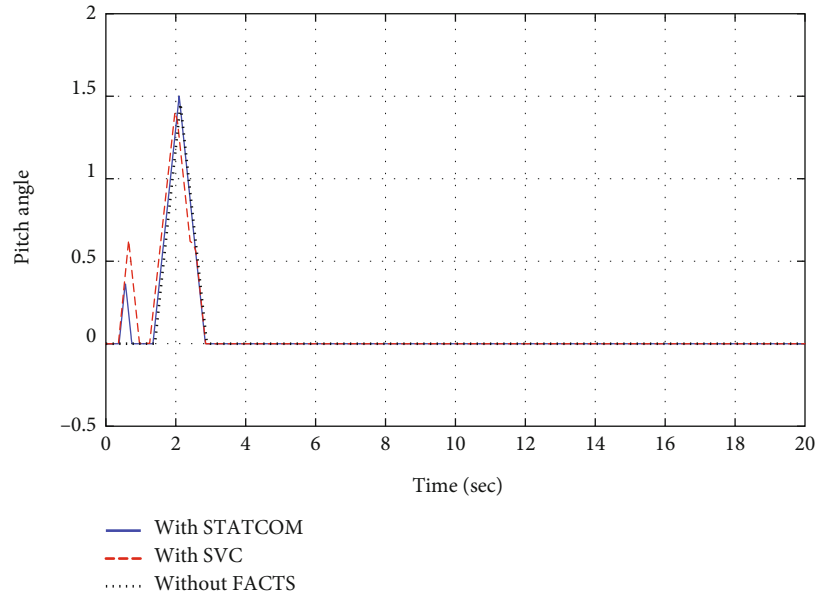


FIGURE 24: Pitch angle control response.

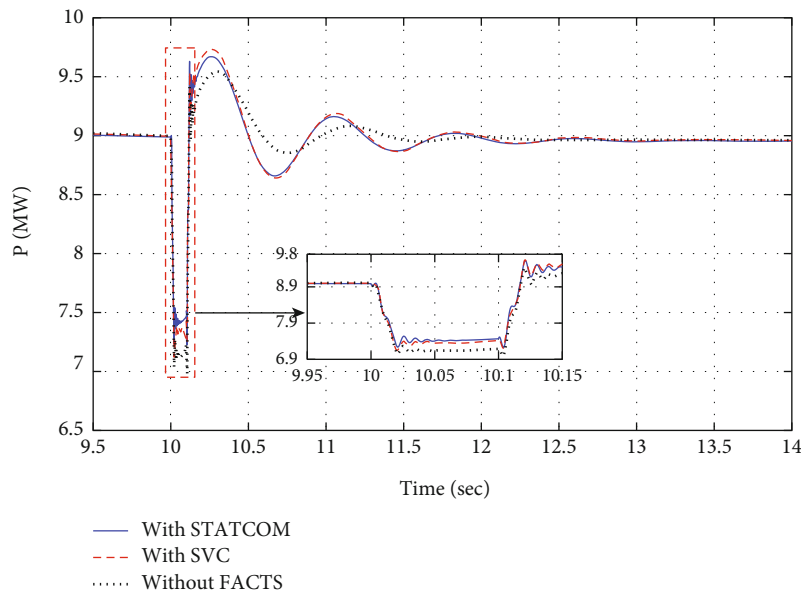


FIGURE 25: Active power at the PCC.

provide a fixed cost figure for the FACTS facility [50]. The approximate purchase and installation costs are given in Table 5 for the given sizes of FACT devices. Moreover, the price of the SVC is lower than the price of STATCOM by 33.33% for the same rated MVAR.

4. Discussion of Simulated Results

Different simulations are carried out where both normal activity and grid failure were assessed to examine the response of the models listed under different working conditions. The main purpose of the voltage sags and wind speed variability is demonstrated in five case studies to examine the FACTS' ability to overwhelm these faults and boost the WF's efficiency

when facing disturbances. It permits the simulation of a transient fault on the PCC because of grid disruptions, tracking the impact on the WF and demonstrating the changes made with the FACTS integration as wanted. Hence, since these faults are assumed to occur in the power grid, the PCC is the place selected to present the disturbance. A comparison between the fixed capacitor, SVC, and STATCOM is presented under five scenarios: (1) high turbulent wind speed, (2) low turbulent wind speed profile, (3) single-phase fault, (4) line-to-line faults, and (5) three-phase fault. Moreover, these scenarios have been done to study their effect on FRT capability.

4.1. Case Study 1: High Turbulent Wind Speed Profile. Random and rapid changes in wind speed make wind an irregular and

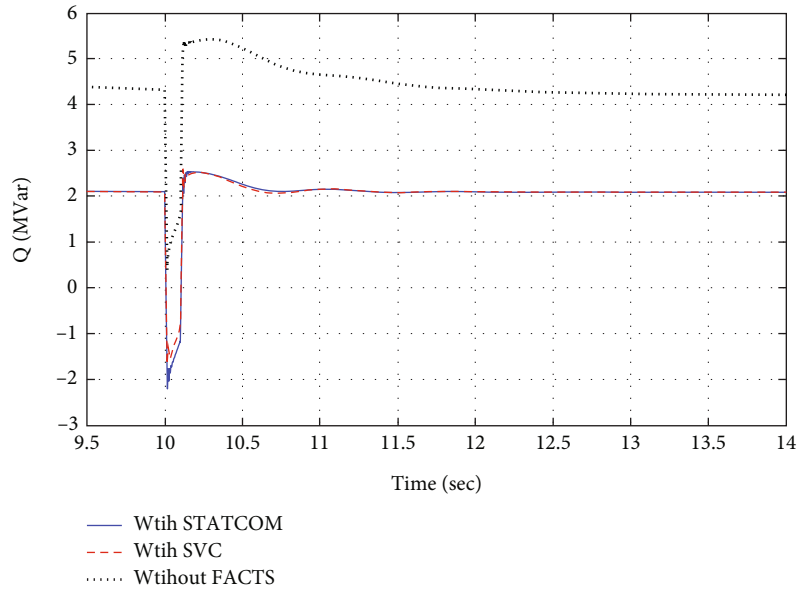


FIGURE 26: The Q at the PCC.

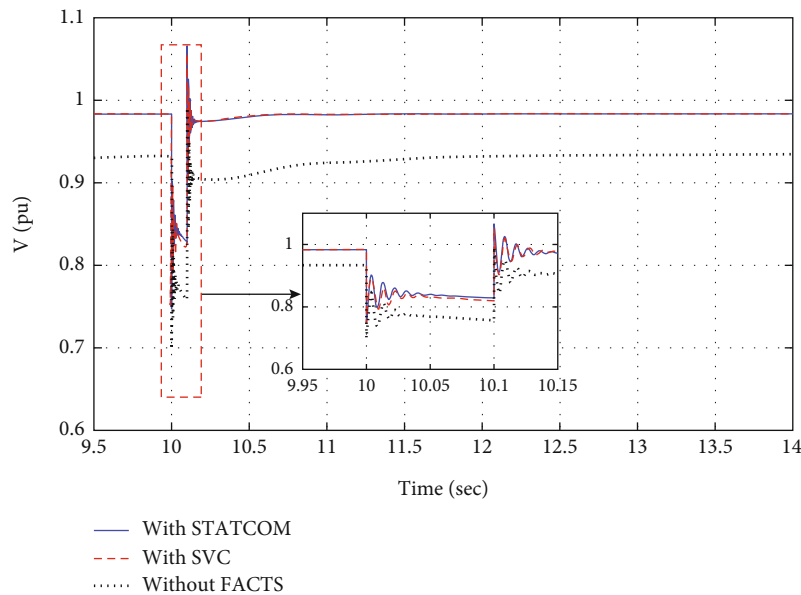


FIGURE 27: Voltage response at the PCC.

inconsistent power source. FACTS devices are one of the most effective solutions for this issue. The SVC and STATCOM are used in this study to compensate for the Q, improve the voltage fluctuation, and improve the system stability. The simulation results show that SVC is superior compared to fixed capacitors and STATCOM due to its high rate. Unfortunately, a fixed capacitor is unable to realize voltage stability and trips the WF from the grid after five seconds due to the shortage of Q. This leads to a drop in voltage and then over current relay turn on to give the order for circuit breakers (CB) to take a decision. The simulated results indicate that voltage improvement with SVC is compared to the other devices because of the high rate for SVC compared to others. Figure 7 shows the high turbulent wind speed where a small interval of the figure is enlarged to

show the severe changes in the wind speed. The active power transfer from the WF to the grid is illustrated in Figure 8. Here, the SVC and STATCOM scenarios are oscillating around 9 MW (the total power of WF). However, in the “without FACTS” case, the WF is cut off because the system cannot repair this problem so the total power of the WF equals zero. Meanwhile, Figure 9 presents the Q_g at the PCC both for the SVC and STATCOM cases, when these devices inject Q into the system. But, in the “without FACTS” case, the system cannot keep on the WF, so the depicted Q is equal to the value of Q generated from the fixed capacitors, i.e., around 1.2 MVAR (400 kVAR for each unit).

Both FACTS devices are able to realize FRT capability, but SVC presents better voltage during transient compared

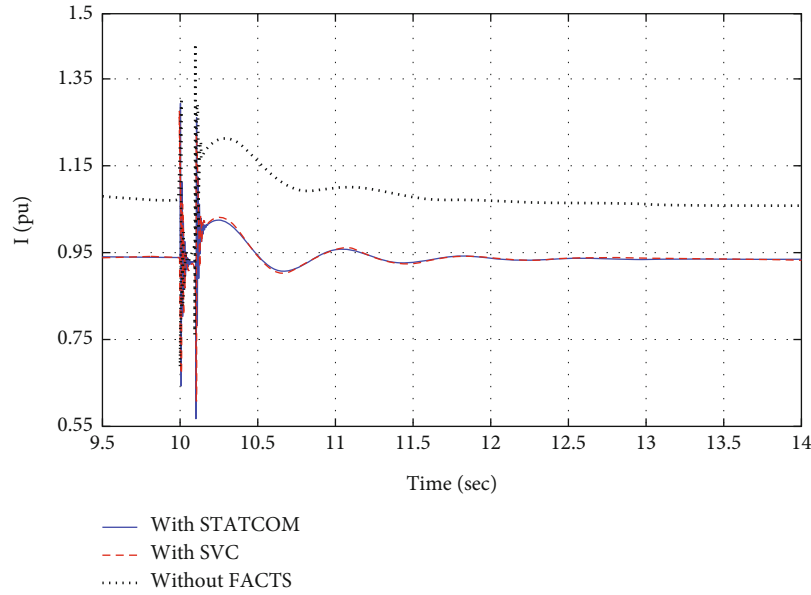


FIGURE 28: The response of the system current.

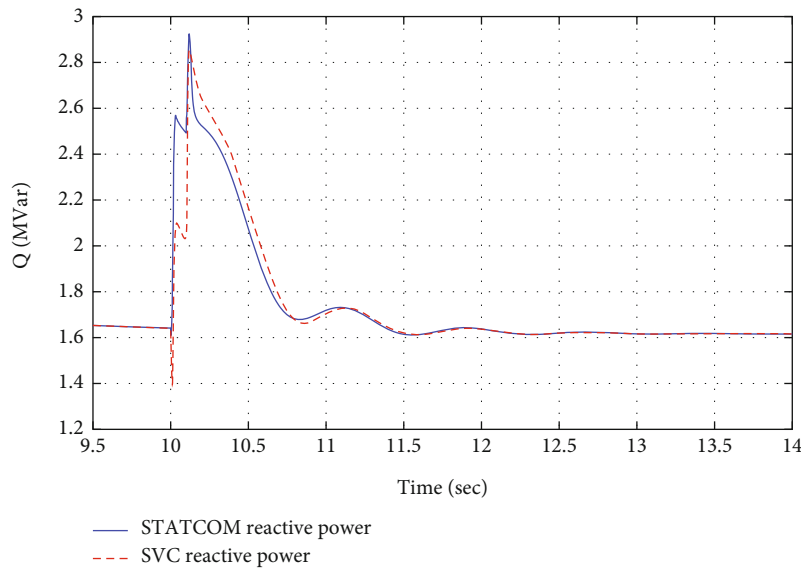


FIGURE 29: The Q of SVC and STATCOM.

to STATCOM and that is due to the highly rated SVC device. The voltage response of the system at the PCC is presented in Figure 10. In the case of “without FACTS,” the voltage is becoming more than the reference value after the WF is cut off and the FRT capability is not achieved. Figures 11–13 depict the system current, the Q of SVC and STATCOM, and the voltage of SVC and STATCOM, respectively. These show that the SVC achieves a little more improvement than STATCOM, but both of them improve the voltage quality.

The SVC and STATCOM can help to mitigate the SCIG speed variation and keep them in the service as depicted in Figure 14, in contrast to the “without FACTS” case where

the WF is out of service. The pitch angle control is activated to help the WF as illustrated in Figure 15.

4.2. Case Study 2: Low Turbulent Wind Speed Profile. The second scenario examines the response of SVC and STATCOM in the case of realistic wind speed and their ability to overcome this issue, mitigate the voltage fluctuation, and achieve the FRT capability besides keeping the system in stable mode and keeping the WF in service. Figure 16 shows the realistic wind speed. Figure 17 shows the total active power injected into the grid from the wind farm. It is obvious that in all cases the WF is still in service. The Q response is shown in Figure 18, where the less injected Q from the

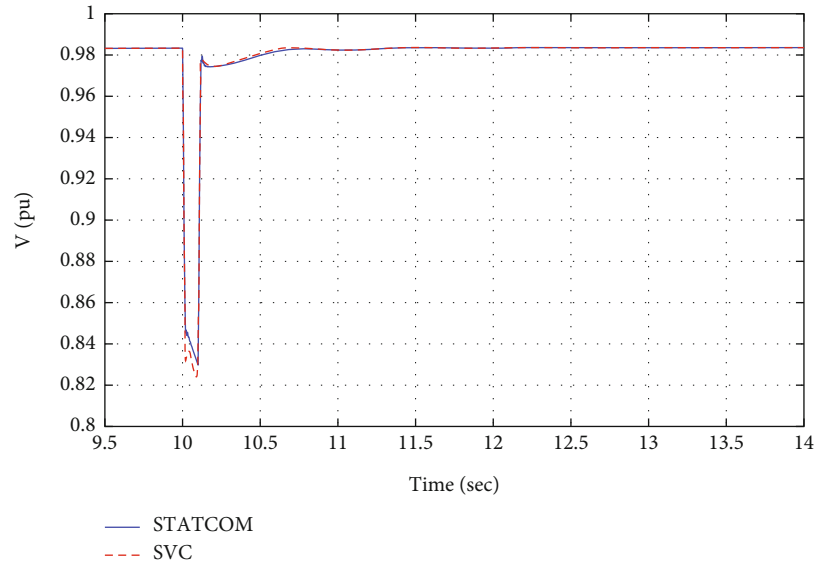


FIGURE 30: The voltage of SVC and STATCOM.

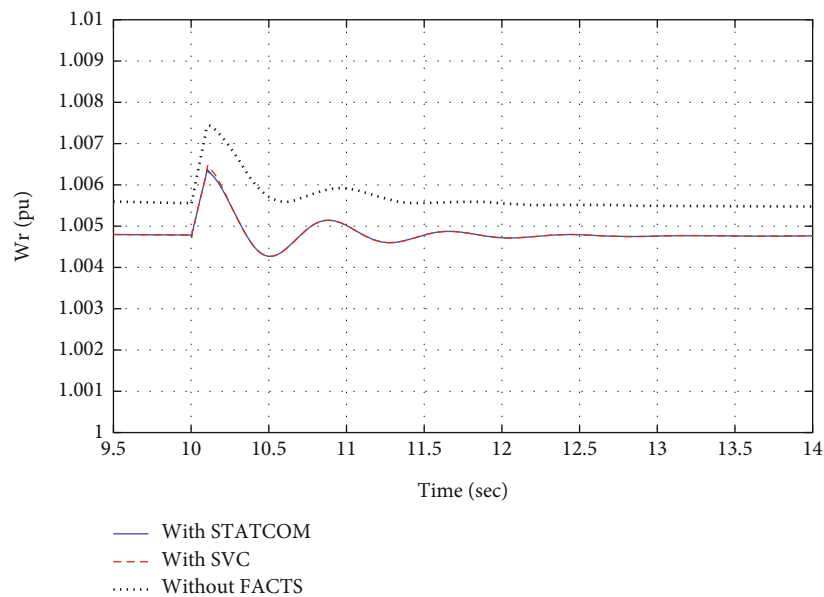


FIGURE 31: SCIG speed variation.

grid is achieved in cases of using SVC and STATCOM, and the largest Q is injected from the grid to the WF in the case of “without using FACTS.”

Voltage can reach the steady state in the case of SVC faster than in the case of STATCOM, and it has a better performance during the overall simulation period and achieve the LVRT capability. In the case of using STATCOM, the voltage response is better than in the case without FACTS and achieves the LVRT capability. The voltage and current response of the studied system is presented in Figures 19 and 20, respectively. Figures 21 and 22 depict the Q supplied from the SVC and STATCOM and the voltage response for both devices, respectively, where the SVC has a better performance than STATCOM.

The good performance for the SVC and STATCOM leads to the improvement of the SCIG speed response as shown in Figure 23, while the control of pitch angle is operated at the transient period because the WF has been exposed to wind speed over its rated value which equals 9 m.s^{-1} during this period that has been depicted in Figure 24.

4.3. Case Study 3: FRT Capability Realization during Single-Phase Fault at the PCC. Faults to the ground are other forms of irregular circumstances that may have to be tackled by grid-connected WF. A single-phase ground fault has been considered in this scenario from 10 s to 10.1 s at WF output terminals. When the single-phase fault is applied to the system, a sudden drop will occur in the system components.

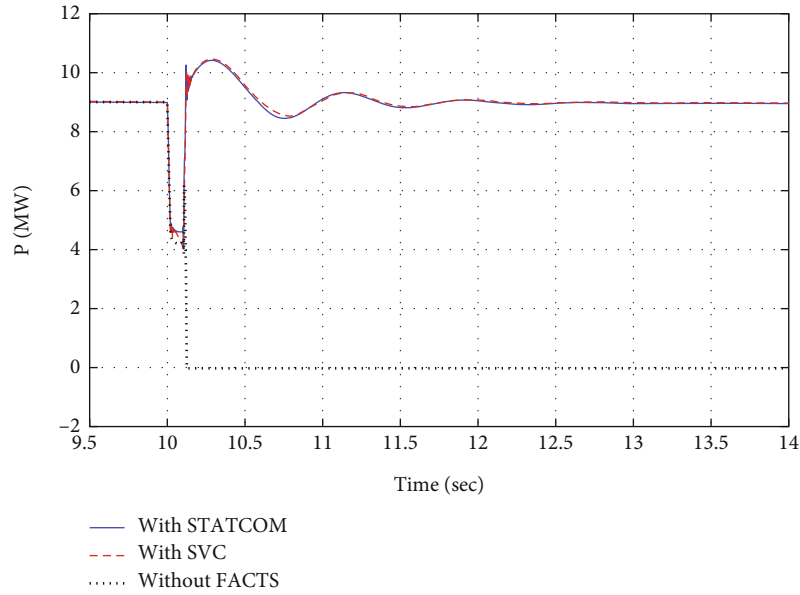


FIGURE 32: Active power at the PCC.

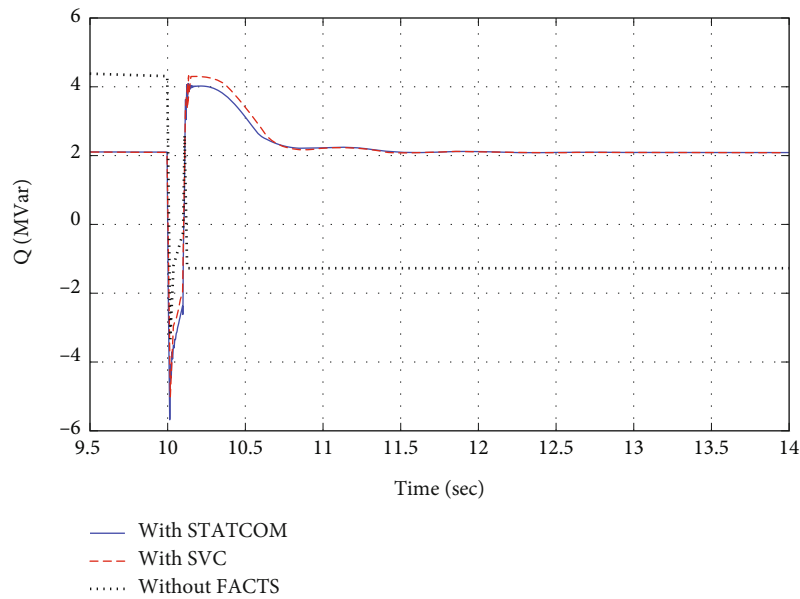


FIGURE 33: The Q at the PCC.

Consequently, the output power of the WF will decrease suddenly from 10s until 10.1 s, as shown in Figure 25. It is obvious that the presence of FACTS helps to mitigate the active power of the WF during the fault period. The Q injected from the grid is reduced in the presence of SVC and STATCOM, as presented in Figure 26. This helps to enhance the voltage response during the fault and the steady-state period as shown in Figure 27 and achieve FRT capability.

The response of the system current is illustrated in Figure 28: the current drawn from the grid is reduced in cases of using SVC and STATCOM. The behavior of SVC and

STATCOM concerning the Q and voltage response for each case is presented in Figures 29 and 30, respectively. The SCIG speed variation is shown in Figure 31.

4.4. Case Study 4: FRT Capability Realization during Two-Phase Fault at the PCC. This type of fault may occur and causes the WF to trip from the grid, which is not allowable according to new grid codes. In this study, a comparison between the responses of SVC and STATCOM has been done to present the ability of these devices to overcome the two-phase fault. The duration of fault is performed between 10s and 10.1s. The STATCOM and SVC have the ability to

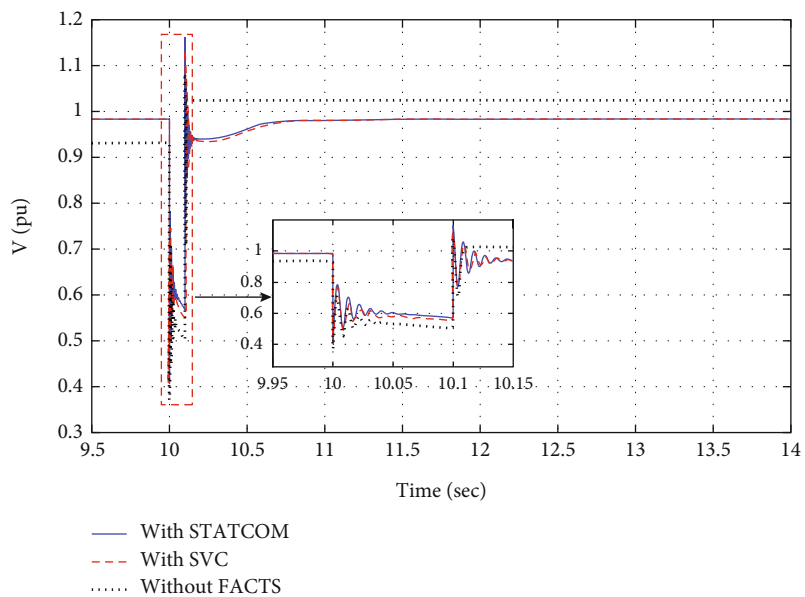


FIGURE 34: Voltage response at the PCC.

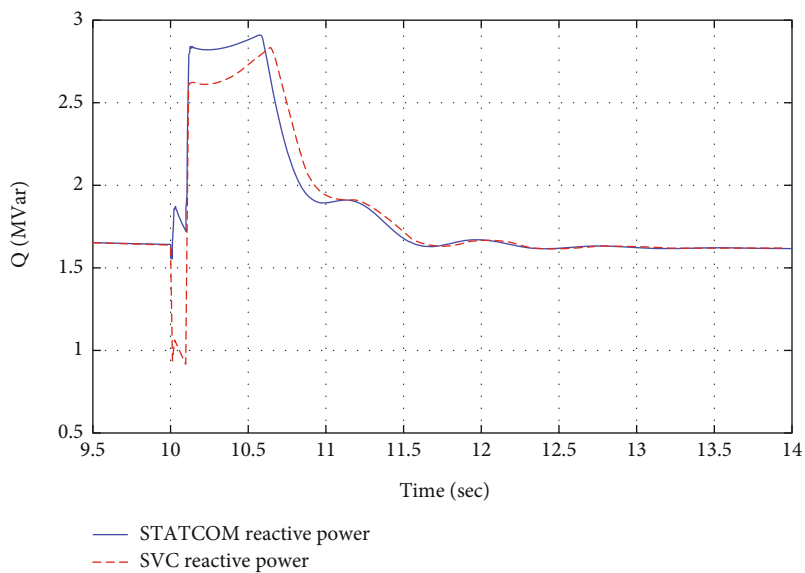


FIGURE 35: The Q of SVC and STATCOM.

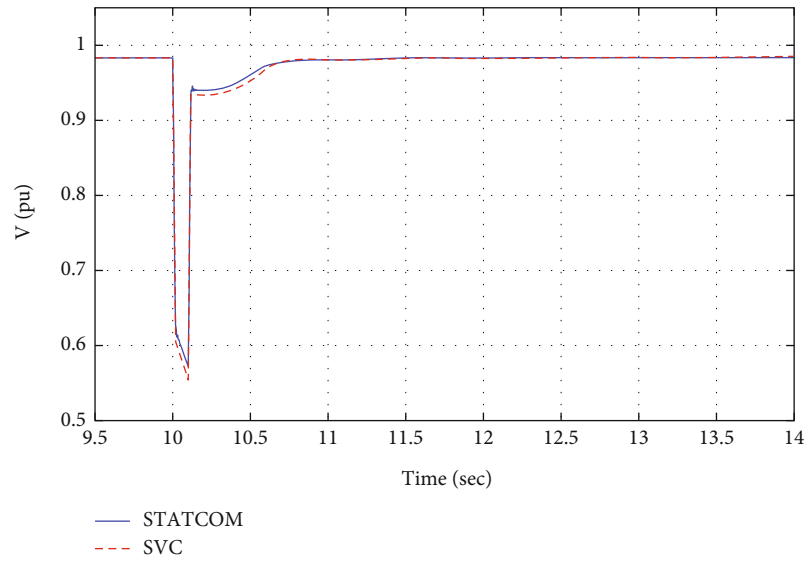


FIGURE 36: A voltage of SVC and STATCOM.

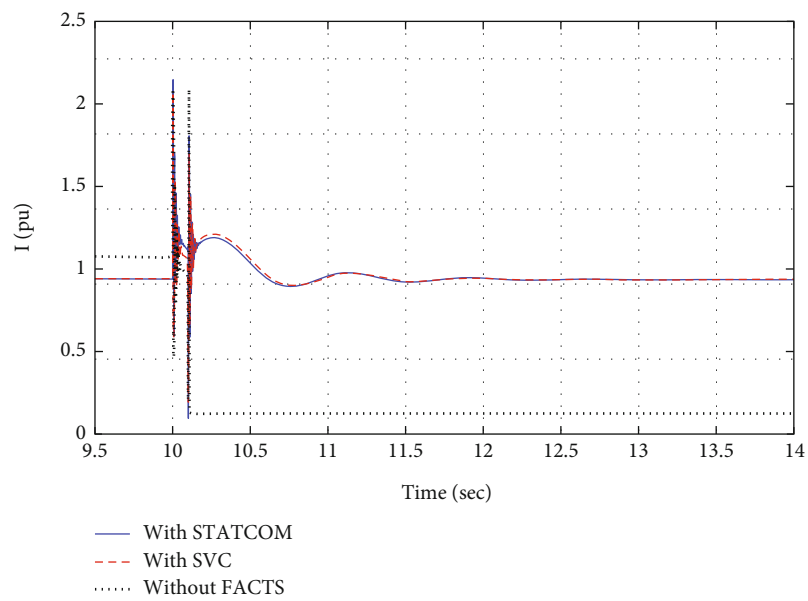


FIGURE 37: The response of the system current.

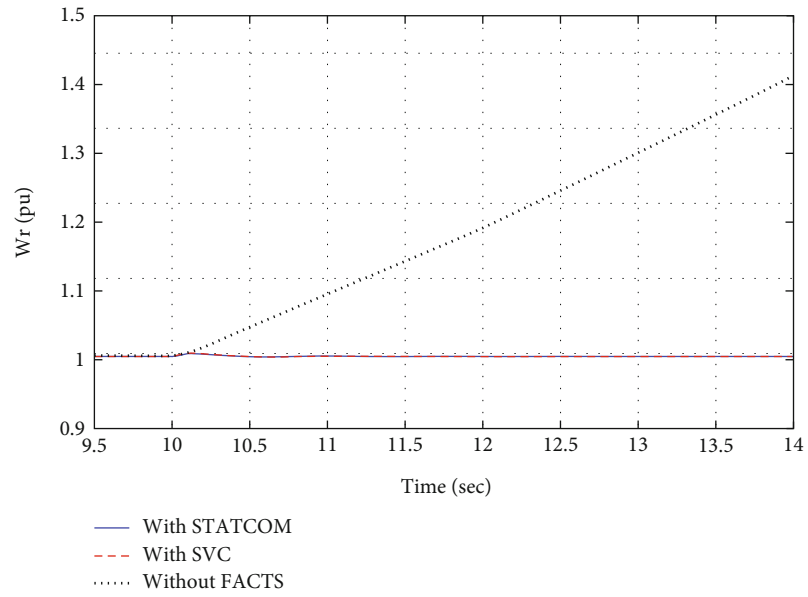


FIGURE 38: SCIG speed variation.

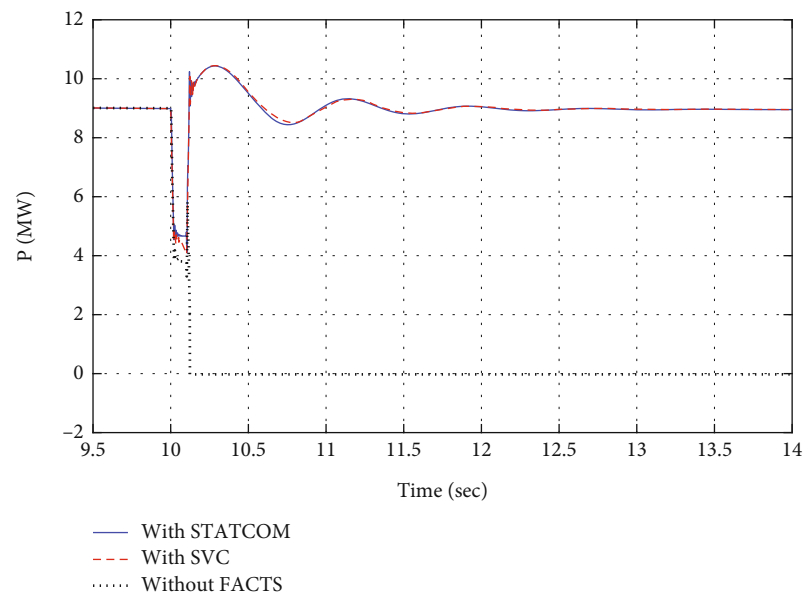


FIGURE 39: Active power at the PCC.

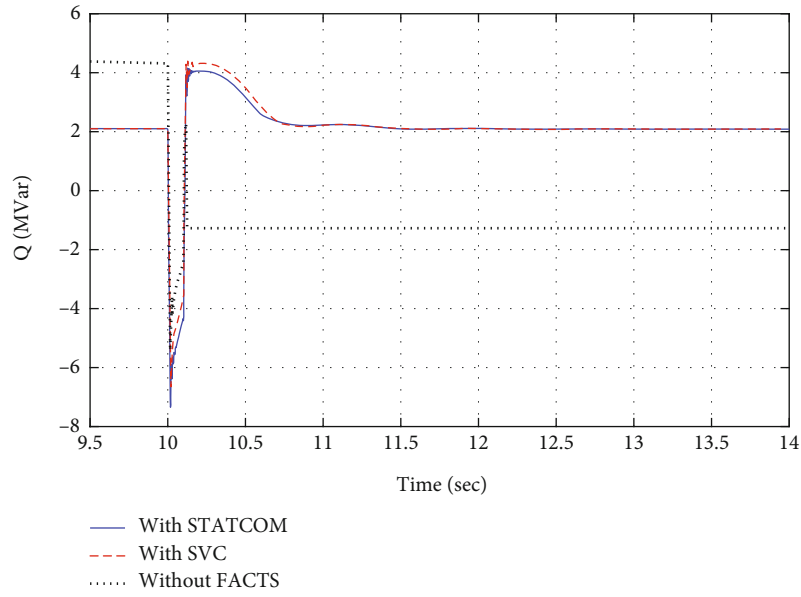


FIGURE 40: The Q at the PCC.

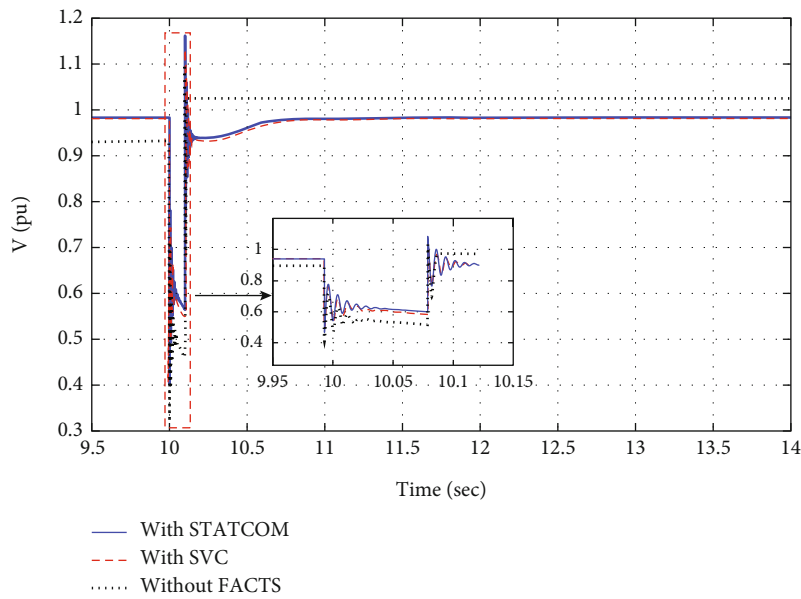


FIGURE 41: Voltage response at the PCC.

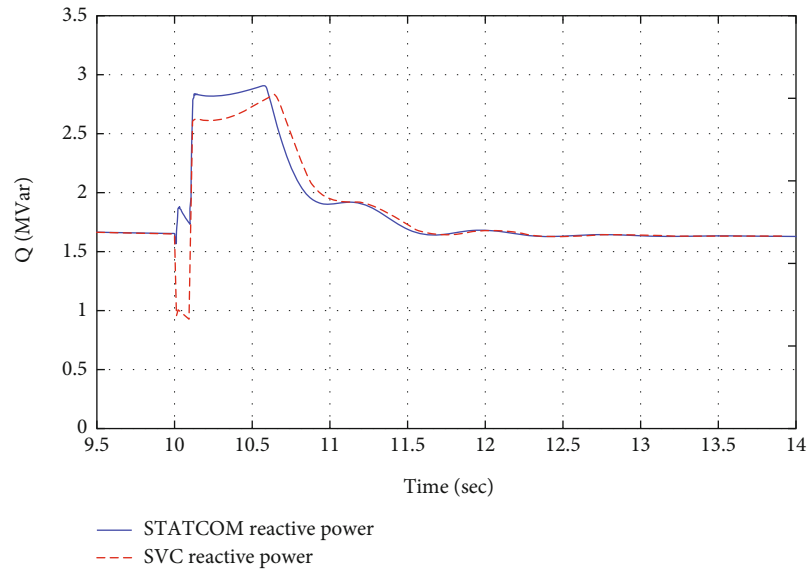


FIGURE 42: The Q of SVC and STATCOM.

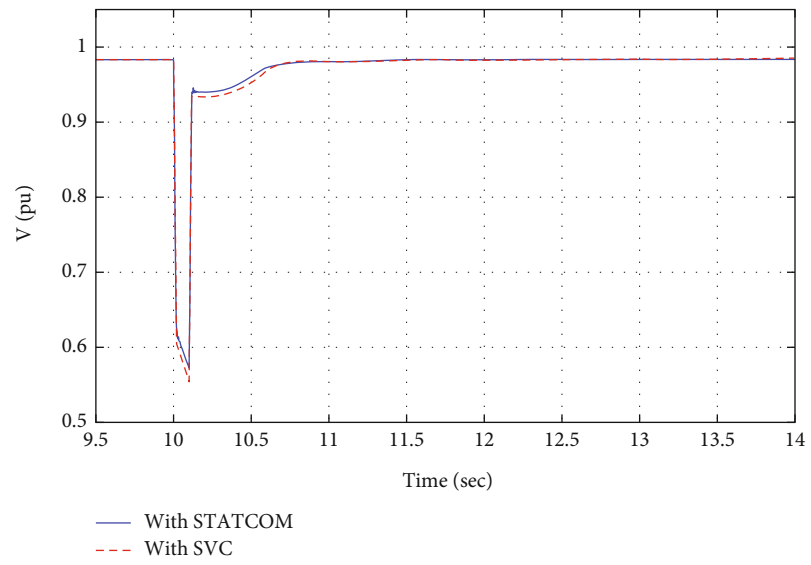


FIGURE 43: A voltage of SVC and STATCOM.

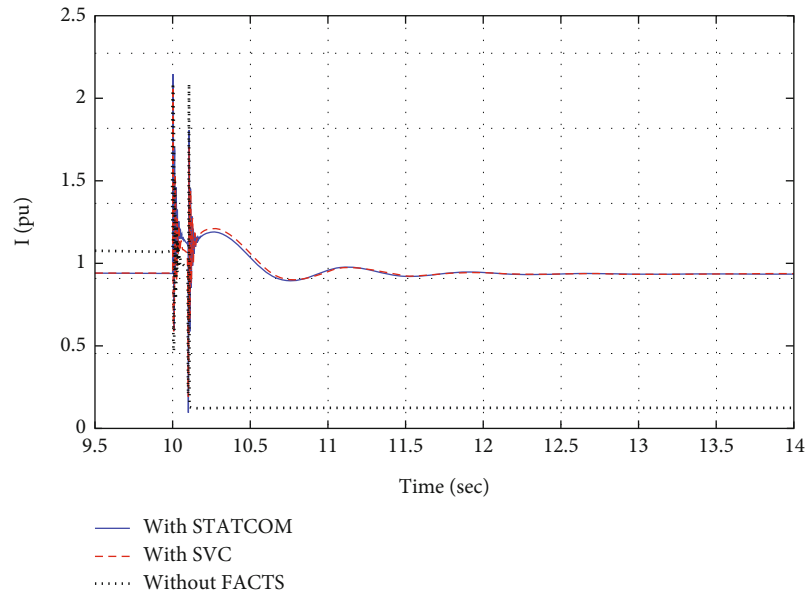


FIGURE 44: The response of the system current.

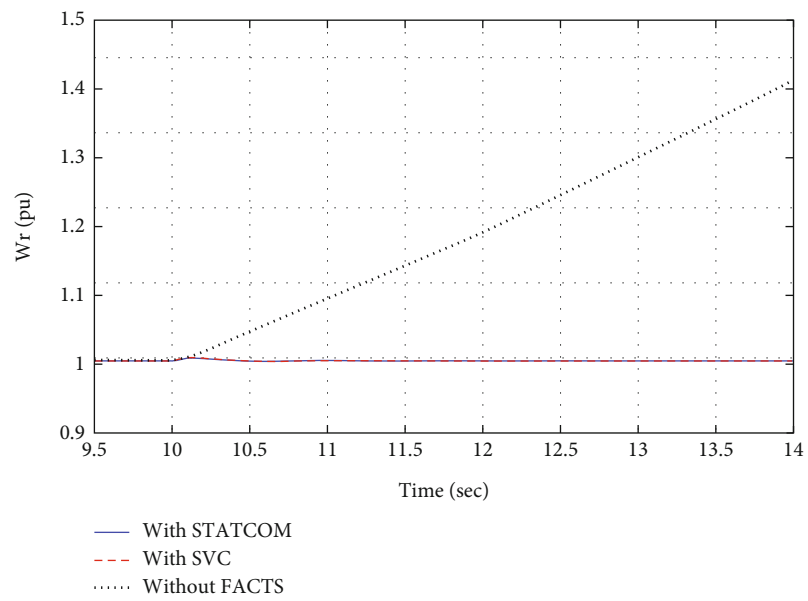


FIGURE 45: SCIG speed variation.

TABLE 6: Overall comparison.

Studied cases	WF in service	The voltage at the PCC	Q_g from the grid	FRT capability	
High turbulent wind speed	Without FACTS	No	Out off-limit before disconnecting the WF	It has the highest value before disconnecting the wind farm	—
	SVC (proposed)	Yes	Recovering is very fast (≈ 1 pu)	It has the lowest value during the overall period	—
	STATCOM	Yes	Recovering is slow (≈ 0.96 pu)	It has a high value during the overall period	—
Low turbulent wind speed	Without FACTS	Yes	It has the worst performance (≈ 0.92 pu)	It has the highest value during the overall period	—
	SVC (proposed)	Yes	It has the best performance (≈ 1 pu)	It has the lowest value during the overall period	—
	STATCOM	Yes	It has an acceptable performance (≈ 0.98 pu)	It has a medium value during the overall period	—
Single-phase fault	Without FACTS	Yes	It has the worst performance	It has the highest value during the overall period	✓
	SVC (proposed)	Yes	It has an acceptable performance	It has a profile approximately equal to the STATCOM case	✓
	STATCOM	Yes	It has the best performance	It has a profile approximately equal to the SVC case	✓
Two-phase fault	Without FACTS	No	It has the worst performance	It has the highest value during the overall period	×
	SVC (proposed)	Yes	It has an acceptable performance	It has a profile high a little compare to the STATCOM case	✓
	STATCOM	Yes	It has the best performance	It has a profile low a little compare to the SVC case	✓
Three-phase fault	Without FACTS	No	It has the worst performance	It has the highest value during the overall period	×
	SVC (proposed)	Yes	It has an acceptable performance	It has a profile high a little compare to the STATCOM case	✓
	STATCOM	Yes	It has the best performance	It has a profile low a little compare to the SVC case	✓

achieve continuous operation for WF during a two-phase fault as shown in Figure 32. But in the “without FACTS” case, the WF is out of service and the output power equals zero. The reactive power supported by the grid is shown in Figure 33 when the grid injects Q into the WF because the WF is still in service. However, in the “without FACTS” case, the grid absorbs the Q generated from the fixed capacitor because the WF is out of service. The FRT capability is achieved by using the STATCOM and SVC during the two-phase fault event as shown in Figure 34. That is because the SVC and STATCOM inject Q to the grid as shown in Figure 35; the voltage response for the SVC and STATCOM is presented in Figure 36. It is obvious that the STATCOM has a bit better performance than SVC because the STATCOM depends on the IGBT switch; meanwhile, the SVC depends on the SCR switch. The response of the system current and SCIG speed variation is shown in Figures 37 and 38, respectively.

4.5. Case Study 5: FRT Capability Realization during Three-Phase Fault at the PCC. The three-phase fault event is considered one of the more dangerous events which threaten the stability of the power system. The overall system components that are affected by a three-phase fault will be discon-

nected from the service and the overall system may collapse. So, in this section, the STATCOM and SVC are examined to overcome the three-phase fault and restore the WF operation, while keeping the power system stable and readable. The duration of the three-phase fault starts at 10 s and ends at 10.1 s. The three-phase fault event causes the WF to get out of service, and the output power reaches zero in the absence of FACTS devices as shown in Figure 39. But when STATCOM and SVC are installed, the WF is still in service, keeping the system stable and reliable. The Q response is illustrated in Figure 40: before the three-phase fault, the amount of Q supplied by the grid to the system is reduced, because STATCOM and SVC injected Q into the system. Moreover, after the three-phase fault, when no FACTS are applied, Q has been injected into the grid equal to 1.2 MVAR which is the sum of the three 400 kVAR by a fixed capacitor because the WF is out of service. But when using STATCOM and SVC, the WF is still in service and consumes Q .

As a result of keeping the WF in service and injecting Q into the grid from the STATCOM and SVC, the FRT capability is achieved: the voltage response is shown in Figure 41. That happens because STATCOM and SVC supplied Q as presented in Figure 42. Voltage response is shown in Figure 43.

STATCOM has a better response than SVC. The system current and SCIG speed variation are shown in Figures 44 and 45, respectively. Table 6 illustrates a comparison between the five studied scenarios.

5. Conclusion

This paper aims at improving the relationship between FSWG and the power grid via the implementation of SVC and STATCOM. The WF under study comprised three similar sections with double 1.5 MW SCIG linked to each and a compensating capacitor of 400 kVAR for each pair of SCIG. Two different FACTS are well-thought-out, i.e., STATCOM and SVC connected to the production terminals of the WF. Five different scenarios were performed, including normal operating conditions (wind speed changing) and abnormal operating events (grid faults). The efficiency and effectiveness of the two suggested FACTS have been assessed and compared to those without any compensating system under the studied scenarios. Simulation results prove that all of the FACTS considered here are capable of improving the dynamic response of FSWG, achieving FRT capability, and boosting voltage stability compared to the base case “without FACTS.” Moreover, to put down the amount of Q needed by the WF from the grid, STATCOM or SVC is installed to support the grid, and under certain conditions, WF voltage can also be adequately supported. SVC and STATCOM at the same rated as MVAR have been implemented and compared under the cases of symmetrical and asymmetrical faults. STATCOM gives better performance compared to SVC. SVC is tested and compared with STATCOM under the two scenarios of wind speed profile. With the proposed SVC system, the obtained simulated results indicate the following:

- (i) The investigated WF can adjust the injected Q while capturing the maximal power during fluctuations in wind speed
- (ii) Due to its high rate and ability to maintain the voltage at ≈ 1 pu, it outperformed fixed capacitors and STATCOM under the high turbulent wind speed profile. Unfortunately, a fixed capacitor cannot achieve voltage stability and, after five seconds, trips the WF from the grid due to a lack of Q
- (iii) The implemented SVC outperformed STATCOM and the fixed capacitor for a low turbulent wind speed profile and successfully maintained the voltage at ≈ 1 pu. In this situation, the other instruments perform satisfactorily, especially STATCOM, which maintained the voltage at ≈ 0.98 pu
- (iv) SVC and STATCOM both outperform fixed capacitors in fault circumstances and achieve FRT in 0.12 seconds. Only when there is a single-phase fault does the fixed capacitor achieve FRT; all other analyzed fault conditions fail

- (v) Its control method reacts to the imbalance between mechanical and generated active power during the fault period. Without requiring any adjustments to the prefault set point of the Q, it injects the needed Q into the grid to preserve its voltage
- (vi) The amount of Q that is injected is directly proportional to voltage sag (period/amplitude). It is reverse proportional to the prefault levels
- (vii) As the rotor speed gradually returns to its initial state once the fault has been removed, the WF-produced active power also gradually rises
- (viii) The rising in the values of the rotor speed is based on the voltage sag magnitude and period (direct proportional)

In conclusion, it is obvious that the SVC, with its straightforward control strategy, can efficiently achieve the FRT capability and voltage stability and allow the WF to obtain the maximum permitted wind power in both healthy and faulty events without requiring any additional complex control techniques, which consequently results in increasing the system efficiency and the life span of the WF and enables the high penetration scenarios for this renewable generator.

Data Availability

The data used to support the findings of the study are available on request from the corresponding author.

Conflicts of Interest

The authors declare that they have no conflicts of interest.

References

- [1] International Renewable Energy Agency, *Renewable capacity highlights*, Irena, 2021.
- [2] M. S. Liang, G. H. Huang, J. P. Chen, and Y. P. Li, “Development of non-deterministic energy-water-carbon nexus planning model: a case study of Shanghai, China,” *Energy*, vol. 246, p. 123300, 2022.
- [3] M. M. Mahmoud, M. M. Aly, and A. M. M. Abdel-Rahim, “Enhancing the dynamic performance of a wind-driven PMSG implementing different optimization techniques,” *SN Applied Sciences*, vol. 2, no. 4, pp. 1–19, 2020.
- [4] M. Abdulhamid and K. Benard, “Study of stability analysis of power system with increasing wind power,” *International Review of Applied Sciences and Engineering*, vol. 11, pp. 1–3, 2020.
- [5] R. Hiremath and T. Moger, “Comprehensive review on low voltage ride through capability of wind turbine generators,” *International Transactions on Electrical Energy Systems*, vol. 30, no. 10, 2020.
- [6] S. M. Rashid, E. Akbari, F. Khalafian, M. H. Atazadegan, S. Shahmoradi, and A. Z. G. Seyyedi, “Robust allocation of FACTS devices in coordinated transmission and generation expansion planning considering renewable resources and demand response programs,” *International Transactions on*

- Electrical Energy Systems*, vol. 2022, article 4331293, pp. 1–16, 2022.
- [7] R. M. M. Pereira, C. M. M. Ferreira, and F. P. M. Barbosa, “Comparative study of STATCOM and SVC performance on dynamic voltage collapse of an electric power system with wind generation,” *IEEE Latin America Transactions*, vol. 12, no. 2, pp. 138–145, 2014.
- [8] J. Joshi, A. K. Swami, V. Jatelly, and B. Azzopardi, “A comprehensive review of control strategies to overcome challenges during LVRT in PV systems,” *IEEE Access*, vol. 9, pp. 121804–121834, 2021.
- [9] A. Sisay and V. Jatelly, “Dynamic performance of grid-connected wind farms with and without UPFC: a case study on Ashagoda wind farm,” *Advances in Intelligent Systems and Computing*, vol. 989, pp. 559–568, 2020.
- [10] A. Sukhnandan, A. K. Saha, and B. Rigby, “A Case Study of Voltage Stability Challenges (on a Unique Utility-Scale System in a Developing African Country),” in *2021 International Conference on Advances in Electrical, Computing, Communication and Sustainable Technologies (ICAECT)*, Bhilai, India, 2021.
- [11] A. W. Kumar, M. U. Mufti, and M. Y. Zargar, “Adaptive predictive control of flywheel storage for transient stability enhancement of a wind penetrated power system,” *International Journal of Energy Research*, vol. 46, no. 5, pp. 6654–6671, 2022.
- [12] P. V. Vardhan Varma and B. Kalyan Kumar, “New unified NR power flow algorithm for initialising fixed speed wind generation system with turbine characteristics,” *IET Renewable Power Generation*, vol. 13, no. 10, pp. 1761–1769, 2019.
- [13] H. M. I. Alkafrawi, T. R. S. Al Aga, Y. S. A. Shaheen, I. M. Elkafrawi, and H. S. A. Ben Abdelmula, “Indirect vector control of squirrel-cage induction generator,” *Journal of Engineering Research and Reports*, vol. 22, no. 1, pp. 23–32, 2022.
- [14] M. M. Mahmoud, M. K. Ratib, M. M. Aly, A. Moamen, and M. A. Rahim, “Effect of grid faults on dominant wind generators for electric power system integration: a comparison and assessment,” *Energy Systems Research*, vol. 4, no. 3, pp. 70–78, 2021.
- [15] M. Bajaj and A. K. Singh, “Grid integrated renewable DG systems: a review of power quality challenges and state-of-the-art mitigation techniques,” *International Journal of Energy Research*, vol. 44, no. 1, pp. 26–69, 2020.
- [16] X. Yin, “An up to date review of continuously variable speed wind turbines with mechatronic variable transmissions,” *International Journal of Energy Research*, vol. 42, no. 4, pp. 1442–1454, 2018.
- [17] K. Reddy and A. K. Saha, “A review of swarm-based metaheuristic optimization techniques and their application to doubly fed induction generator,” *Heliyon*, vol. 8, no. 10, article e10956, 2022.
- [18] M. M. Mahmoud, “Improved current control loops in wind side converter with the support of wild horse optimizer for enhancing the dynamic performance of PMSG-based wind generation system,” *International Journal of Modelling and Simulation*, pp. 1–15, 2022.
- [19] M. M. Mahmoud, M. K. Ratib, M. M. Aly, and A. M. M. Abdel-Rahim, “Application of whale optimization technique for evaluating the performance of wind-driven PMSG under harsh operating events,” *Process Integration and Optimization for Sustainability*, vol. 6, no. 2, pp. 447–470, 2022.
- [20] M. M. Mahmoud, M. Khalid Ratib, M. M. Aly, and A. M. M. Abdel-Rahim, “Wind-driven permanent magnet synchronous generators connected to a power grid: existing perspective and future aspects,” *Wind Engineering*, vol. 46, no. 1, pp. 189–199, 2022.
- [21] A. Akinrinde, A. Swanson, and R. Tiako, “Dynamic behavior of wind turbine generator configurations during ferroresonant conditions,” *Energies*, vol. 12, no. 4, p. 639, 2019.
- [22] L. M. Fernández, J. R. Saenz, and F. Jurado, “Dynamic models of wind farms with fixed speed wind turbines,” *Renewable Energy*, vol. 31, no. 8, pp. 1203–1230, 2006.
- [23] F. Sulla, J. Svensson, and O. Samuelsson, “Symmetrical and unsymmetrical short-circuit current of squirrel-cage and doubly-fed induction generators,” *Electric Power Systems Research*, vol. 81, no. 7, pp. 1610–1618, 2011.
- [24] H. Li, B. Zhao, C. Yang, H. W. Chen, and Z. Chen, “Analysis and estimation of transient stability for a grid-connected wind turbine with induction generator,” *Renewable Energy*, vol. 36, no. 5, pp. 1469–1476, 2011.
- [25] J. M. Rodríguez, J. L. Fernández, D. Beato et al., “Incidence on power system dynamics of high penetration of fixed speed and doubly fed wind energy systems: study of the Spanish case,” *IEEE Transactions on Power Apparatus and Systems*, vol. 17, no. 4, pp. 1089–1095, 2002.
- [26] Y.-K. Wu, S.-M. Chang, and P. Mandal, “Grid-connected wind power plants: a survey on the integration requirements in modern grid codes,” *IEEE Transactions on Industry Applications*, vol. 55, no. 6, pp. 5584–5593, 2019.
- [27] T. R. Ayodele, A. A. Jimoh, J. L. Munda, and J. T. Agee, “Challenges of grid integration of wind power on power system grid integrity: a review,” *International Journal of Renewable Energy Research*, vol. 2, no. 4, pp. 618–626, 2012.
- [28] A. Q. Al-Shetwi, M. A. Hannan, K. P. Jern, M. Mansur, and T. M. I. Mahlia, “Grid-connected renewable energy sources: review of the recent integration requirements and control methods,” *Journal of Cleaner Production*, vol. 253, article 119831, 2020.
- [29] X. Zhang, C. Rehtanz, and B. Pal, *Flexible AC Transmission Systems: Modelling and Control*, Springer Science & Business Media, 2006.
- [30] O. C. C. and O. I. I. Ochi I.S., *International Conference on Engineering Adaptation and Policy Reforms*, pp. 331–337, 2019, <https://www.absradiotv.com/2019/11/08/coou-international-conference-on-engineering-adaptation-and-policy-reforms-for-industrial-development-at-uli-campus/>.
- [31] S. Ushkewar, “Mathematical modelling of STATCOM for reactive power compensation in power system and approach to the renewable energy,” in *Lecture Notes in Electrical Engineering*, vol. 569, pp. 167–174, Springer Verlag, 2020.
- [32] M. Dashtdar, M. Bajaj, S. M. S. Hosseinimoghadam et al., “Improving voltage profile and reducing power losses based on reconfiguration and optimal placement of UPQC in the network by considering system reliability indices,” *International Transactions on Electrical Energy Systems*, vol. 31, no. 11, article e13120, 2021.
- [33] A. Movahedi, A. H. Niasar, and G. B. Gharehpetian, “Designing SSSC, TCSC, and STATCOM controllers using AVURPSO, GSA, and GA for transient stability improvement of a multi-machine power system with PV and wind farms,” *International Journal of Electrical Power & Energy Systems*, vol. 106, pp. 455–466, 2019.

- [34] V. Salehi, S. Afsharnia, and S. Kahrobaee, "Improvement of voltage stability in wind farm connection to distribution network using FACTS devices," in *IECON Proceedings (Industrial Electronics Conference)*, pp. 4242–4247, Paris, France, 2006.
- [35] H. Rezaie and M. H. Kazemi-Rahbar, "Enhancing voltage stability and LVRT capability of a wind-integrated power system using a fuzzy-based SVC," *Engineering Science and Technology, an International Journal*, vol. 22, no. 3, pp. 827–839, 2019.
- [36] Y. K. Gounder, D. Nanjundappan, and V. Boominathan, "Enhancement of transient stability of distribution system with SCIG and DFIG based wind farms using STATCOM," *IET Renewable Power Generation*, vol. 10, no. 8, pp. 1171–1180, 2016.
- [37] A. Luna, P. Rodriguez, R. Teodorescu, and F. Blaabjerg, "Low voltage ride through strategies for SCIG wind turbines in distributed power generation systems," in *PESC Record-IEEE Annual Power Electronics Specialists Conference*, pp. 2333–2339, Rhodes, Greece, 2008.
- [38] D. Ramirez, S. Martinez, F. Blazquez, and C. Carrero, "Use of STATCOM in wind farms with fixed-speed generators for grid code compliance," *Renewable Energy*, vol. 37, no. 1, pp. 202–212, 2012.
- [39] O. Noureldeen, "Low voltage ride through strategies for SCIG wind turbines interconnected grid," *International Journal of Electrical & Computer Sciences*, vol. 11, no. 2, pp. 53–58, 2011.
- [40] A. Arulampalam, M. Barnes, N. Jenkins, and J. B. Ekanayake, "Power quality and stability improvement of a wind farm using STATCOM supported with hybrid battery energy storage," *IEE Proceedings-Generation, Transmission and Distribution*, vol. 153, no. 6, pp. 701–710, 2006.
- [41] S. M. Muyeen, M. H. Ali, R. Takahashi, T. Murata, and J. Tamura, "Wind generator output power smoothing and terminal voltage regulation by using STATCOM/ESS," in *2007 IEEE Lausanne POWERTECH, Proceedings*, pp. 1232–1237, Lausanne, Switzerland, 2007.
- [42] R. Sarrias, C. González, L. M. Fernández, C. Andrés García, and F. Jurado, "Comparative study of the behavior of a wind farm integrating three different FACTS devices," *Journal of Electrical Engineering and Technology*, vol. 9, no. 4, pp. 1258–1268, 2014.
- [43] O. Anaya Lara, N. Jenkins, and J. Ekanayake, *Wind Energy Generation Systems: Modelling and Control*, vol. 54, John Wiley & Sons, 2009.
- [44] I. H. Al-bahadly, *Wind Turbines*, InTech, 2011.
- [45] M. M. Mahmoud, A. M. Hemeida, and A. M. Abdel-Rahim, "Behavior of PMSG wind turbines with active crowbar protection under faults," in *2019 Innovations in Power and Advanced Computing Technologies (i-PACT)*, Vellore, India, 2019.
- [46] E. Acha, C. R. Fuerte-Esquivel, H. Ambriz-Perez, and C. Angeles-Camacho, *FACTS: modelling and simulation in power networks*, John Wiley & Sons, 2004.
- [47] T. Amroune, M. Bourzami, and A. Bouktir, "Improvement of transient stability margin in power systems with integrated wind generation using the SVC," in *13th International conference on Sciences and Techniques of Automatic control & computer engineering*, pp. 1228–1241, Monastir, Tunisia, 2012.
- [48] Y. Wei, L. Kang, R. Qi, M. Wen, and M. M. Cheng, "Optimal control of SVC-MERS and application in SCIG powered micro-grid," in *Conference Proceedings-IEEE Applied Power Electronics Conference and Exposition-APEC*, pp. 3367–3373, Fort Worth, TX, USA, 2014.
- [49] P. Sravanthi, K. R. Rani, J. Amarnath, and S. Kamakshaiah, "Critical clearing time and transient stability analysis of SCIG based wind farm with STATCOM," in *2014 International Conference on Smart Electric Grid (ISEG)*, Guntur, India, 2015.
- [50] F. H. Gandoman, A. Ahmadi, A. M. Sharaf et al., "Review of FACTS technologies and applications for power quality in smart grids with renewable energy systems," *Renewable and Sustainable Energy Reviews*, vol. 82, pp. 502–514, 2018.